Eocene Loranthaceae pollen pushes back divergence ages for major splits in the family

Friðgeir Grímsson[1,*], Paschalia Kapli[2], Christa-Charlotte Hofmann[1], Reinhard Zetter[1] and Guido W. Grimm[1,3,*]

[1] Department of Palaeontology, University of Vienna, Wien, Austria
[2] The Exelixis Lab, Scientific Computing Group, Heidelberg Institute for Theoretical Studies, Heidelberg, Germany
[3] Orléans, France
[*] These authors contributed equally to this work.

ABSTRACT

Background: We revisit the palaeopalynological record of Loranthaceae, using pollen ornamentation to discriminate lineages and to test molecular dating estimates for the diversification of major lineages.
Methods: Fossil Loranthaceae pollen from the Eocene and Oligocene are analysed and documented using scanning-electron microscopy. These fossils were associated with molecular-defined clades and used as minimum age constraints for Bayesian node dating using different topological scenarios.
Results: The fossil Loranthaceae pollen document the presence of at least one extant root-parasitic lineage (Nuytsieae) and two currently aerial parasitic lineages (Psittacanthinae and Loranthinae) by the end of the Eocene in the Northern Hemisphere. Phases of increased lineage diversification (late Eocene, middle Miocene) coincide with global warm phases.
Discussion: With the generation of molecular data becoming easier and less expensive every day, neontological research should re-focus on conserved morphologies that can be traced through the fossil record. The pollen, representing the male gametophytic generation of plants and often a taxonomic indicator, can be such a tracer. Analogously, palaeontological research should put more effort into diagnosing Cenozoic fossils with the aim of including them into modern systematic frameworks.

Subjects Biogeography, Evolutionary Studies, Palaeontology, Plant Science
Keywords Pollen morphology, Pollen as minimum age priors, Uncorrelated clock node dating, Topological uncertainty, Palaeophytogeography, Lineage-through-time plot, Santalales

INTRODUCTION

The Loranthaceae (order Santalales), a moderately large family comprising about 76 genera and over 1,000 species in five tribes (*Nickrent, 1997 onwards*; *Nickrent et al., 2010*), has a wide geographical distribution. Today, there is a relatively clear geographic split between a New World group (Psittacanthinae) and Old World-Australasian lineages (Elythrantheae and Lorantheae), which gave rise to the hypothesis that the initial Loranthaceae diversification was linked to the final phase of the Gondwana breakup in the

Submitted 16 December 2016
Accepted 4 May 2017
Published 7 June 2017

Corresponding authors
Friðgeir Grímsson,
fridgeir.grimsson@univie.ac.at
Guido W. Grimm,
grimmiges@gmail.com

Academic editor
Kenneth De Baets

Additional Information and Declarations can be found on page 39

DOI **10.7717/peerj.3373**

Late Cretaceous (e.g. *Barlow, 1990*; *Vidal-Russell & Nickrent, 2007*). Only three of the more than 70 genera are root parasites and the rest are aerial branch parasites. Molecular studies on Loranthaceae (and Santalales in general) have thus focused on three issues: (1) clarifying the evolutionary relationships within the family (*Vidal-Russell & Nickrent, 2008a*); (2) explaining the transition from root to aerial parasitism (*Wilson & Calvin, 2006*); (3) dating the time of transition to aerial parasitism (*Vidal-Russell & Nickrent, 2008b*). All molecular studies using outgroups recognised the south-western Australian, root-parasitic, monotypic *Nuytsia* R. Br. (monogeneric tribe Nuytsieae; *Nickrent et al., 2010*) as the first diverging lineage in the family (*Wilson & Calvin, 2006*; *Vidal-Russell & Nickrent, 2008a*; *Su et al., 2015*). The other two Loranthaceae root parasites (*Atkinsonia* F. Muell., *Gaiadendron* G. Don; tribe Gaiadendreae) formed a grade to the New World aerial parasites (*Wilson & Calvin, 2006*; multiple origins of aerial parasitism) or all aerial parasitic genera of the family (*Vidal-Russell & Nickrent, 2008a*; *Vidal-Russell & Nickrent, 2008b*; *Su et al., 2015*; singular origin). Using a time-calibrated phylogeny, *Vidal-Russell & Nickrent (2008b)* concluded that Loranthaceae diverged from other Santalales lineages in the uppermost Cretaceous. The first radiation—the divergence of root parasites *Nuytsia*, *Atkinsonia* and *Gaiadendron*—was during the Eocene. The crown age of the aerial parasitic clade within the Loranthaceae, comprising the mostly New World Psittacantheae and Old World-Australasian Erytrantheae and Lorantheae, was placed in the middle Oligocene, approximately 28 Ma (estimated via a Bayesian relaxed clock and fixing the Santalales root to a maximum age of 114 Ma); a time characterised by global cooling (*Zachos et al., 2001*) and retreat of subtropical and tropical vegetation.

Although molecular and morphological interrelationships of Loranthaceae genera are considered now to be relatively clear (*Nickrent et al., 2010*; *Su et al., 2015*; but see *Grímsson, Grimm & Zetter, 2017*), the timing of divergence between the genera has not been cross-checked with available evidence from the fossil record (e.g. *Muller, 1981*; *Song, Wang & Huang, 2004*; *Macphail et al., 2012*). Also, the phytogeographic history of the family is based merely on the present distribution of its genera (e.g. *Vidal-Russell & Nickrent, 2007*) and has not yet been explored in detail (*Vidal-Russell & Nickrent, 2008a*, p. 1027). The latest hypothesis put forward was that Loranthaceae originated when South America, Antarctica and Australia were still connected, and that two large-scale migration events, one from New Zealand and one from Australia, shaped the modern distribution (*Vidal-Russell & Nickrent, 2008a*, *2008b*). The single shift to aerial parasitism was estimated to be of middle Oligocene age. Thus, older fossil records, the oldest going back to the early Eocene (c. 50 Ma) in Australia, were considered to represent root parasites or extinct clades of aerial parasites (*Macphail et al., 2012*).

The outstanding work on the pollen morphology of extant Loranthaceae by *Feuer & Kuijt (1979*, *1980*, *1985)* and other Santalales lineages (*Maguire, Wurdack & Huang, 1974*; *Feuer, 1977*, *1978*, *1981*; *Feuer & Kuijt, 1978*, *1982*; *Feuer, Kuijt & Wiens, 1982*) demonstrated that most pollen produced by members of the Loranthaceae cannot be confused with pollen from other angiosperm families (*Grímsson, Grimm & Zetter, 2017*). *Grímsson, Grimm & Zetter (2017)* distinguished four general types (Pollen Type A, B, C, D),

of which only one (Pollen Type A) could be confused with pollen of other Santalales lineages, and would unlikely be recognised as Loranthaceae pollen if found in a fossil pollen sample. Combined application of light microscopy (LM), scanning-electron microscopy (SEM), and transmission electron microscopy (TEM) revealed that pollen morphologies—including the many variants of B-type pollen—are conserved at various taxonomic levels within Loranthaceae (*Feuer & Kuijt, 1978*, *1979*, *1980*, *1985*; *Caires, 2012*; *Grímsson, Grimm & Zetter, 2017*). Thus, dispersed fossil pollen can aid in the reconstruction of past distributions of Loranthaceae lineages and shed light on the timing of the origin of the modern clades. Being the male gametophyte of a plant, pollen are generally conserved in morphology. Diagnostic (lineage-specific) pollen hence allow for the tracing of modern lineages deep into the past (e.g. *Zetter, Hesse & Huber, 2002*; *Grímsson, Zetter & Hofmann, 2011*; *Grímsson et al., 2016*).

Here, we describe new fossil Loranthaceae pollen grains from the middle Eocene of the United States, Greenland, Central Europe, and East Asia, and from the late Oligocene/early Miocene of Germany. The diagnostic morphological features of the pollen provided sufficient details to assign the fossil pollen to distinct lineages within the Loranthaceae. These fossil pollen represent the earliest unambiguous reports of the root parasitic Nuytsieae, and the presently aerial parasitic lineages Psittacanthinae, Elytrantheae and Lorantheae. Thus, they can be used as potential ingroup minimum age priors for node dating, and to refine our knowledge about the evolutionary history of the Loranthaceae.

MATERIALS AND METHODS

Origin of samples and geological background

The fossil Loranthaceae pollen identified during this study occurred in six different sedimentary rock samples: (1) the Claiborne Group of the Miller Clay Pit in Henry County, Tennessee, United States (sample UF 15817-062117); (2) the Hareøen Formation (middle Eocene) on Qeqertarsuatsiaq Island (Hareøen), western Greenland; (3) the Borkener coal measures of the Stolzenbach underground coal mine, near Kassel, Germany; (4) the Profen Formation (middle Eocene) of the Profen opencast mine, close to Leipzig in Germany; (5) the Changchang Formation (middle Eocene) on northern Hainan Island, South China; (6) the Melker Series of the NÖ05 borehole positioned close to Theiss, near Krems, Lower Austria; and (7) the Cottbus/Spremberg Formations (late Oligocene/early Miocene) of Altmittweida in Saxony, Germany (Table 1). For details on the geographic positions, geology, palaeoecology, and previously known fossil plants from these formations and localities see Table 1 and references therein. Epoch names and ages in Table 1 follow *Cohen et al. (2013* [updated]*)*.

Preparation of samples

The sedimentary rock samples were processed according to the protocols outlined in *Grímsson, Denk & Zetter (2008)*. We investigated the fossil Loranthaceae pollen grains using the 'single grain method' (*Zetter, 1989*), whereby the same fossil pollen grain is first analysed under the LM and then SEM. SEM stubs produced under this study are stored in

Table 1 Information on sample sites.

	Miller Clay Pit MT1–MT3	Aamaruutissaa MT	Stolzenbach MT	Profen MT1–MT5	Changchang MT	Theiss MT	Altmittweida MT
Location	Miller Clay Pit, Henry County, Tennessee, United States	Aamaruutissaa, southeast Hareøen Island, western Greenland	Stolzenbach underground coalmine, Kassel, Germany	Profen opencast mine, close to Leipzig, Germany	Changchang Basin, close to Jiazi Town, Qiongshan County, Hainan, China	Theiss, borehole southeast of Krems, Lower Austria	Altmittweida, Saxony, Germany
Latitude and longitude (ca.)	36°13′N, 88°27′W	70°24′N, 54°41′W	51°0′N, 9°17′E	51°09′N, 12°11′E	19°38′N, 110°27′E	48°23′N, 15°41′E	50°58′N, 12°55′E
Lithostratigraphy	Claiborne Group	Hareøen Formation	Borkener coal measures	Profen Formation	Changchang Formation	Melker Series	Cottbus/ Spremberg Formations
Epoch*	Lutetian	Late Lutetian-early Bartonian	Lutetian	Bartonian	Lutetian-Bartonian	Rupelian	Chattian to Aquitanian
Age (Ma)*	47.8–41.2*	42–40 [absolute dating]	47.8–41.2*	41.2–38*	47.8–37.8*	33.9–28.1*	28.1–20.44*
According to	Litho- and biostratigraphy	Chrono-, litho- and biostratigraphy	Litho- and biostratigraphy	Litho- and biostratigraphy	Litho- and biostratigraphy	Litho- and biostratigraphy	Litho- and biostratigraphy
Notes on palynofloras	Dominated by angiosperms; rich in Fagaceae, Juglandaceae, Sapotaceae, Anarcardiaceae, Olacaceae, Cannabaceae, and Altingiaceae	Diverse spore and pollen flora; rich in Cupressaceae and angiosperms; *Fagus*, *Quercus* and Castaneoideae pollen abundant	Dominated by angiosperms; rich in Ericaceae, Fagaceae, Hamamelidaceae, Altingiaceae, Combretaceae, Burseraceae, Icacinaceae, Juglandaceae, Lecythidiaceae, and Sapotaceae	Dominated by angiosperms; rich in Anacardiaceae, Araceae, Arecaceae, Fagaceae, Sapotaceae, Symplocaceae, and Combretaceae	Diverse in angiosperms; rich in Fagaceae pollen, especially *Quercus* and Castaneoideae	Dominated by angiosperms, rich in Fagaceae, Sapotaceae, Juglandaceae, Vitaceae, Malvaceae, Symplocaceae, Cornaceae, Oleaceae, and Arecaceae	Diverse in angiosperms; rich in Juglandaceae and Fagaceae genera
For further info on the geological background, stratigraphy [S], palaeoenvironment, palaeoclimate, and plant fossils [P]	*Tschudy (1973*[P]*)*; *Potter (1976*[P]*)*; *Taylor (1989*[P]*)*; *Dilcher & Lott (2005*[P/S]*)*; *Wang, Blanchard & Dilcher (2013*[P]*)*	*Heer (1883*[P]*)*; *Hald (1976*, *1977* [S]*)*; *Schmidt et al. (2005*[S]*)*; *Dam et al. (2009*[S]*)*; *Grímsson et al. (2014a*, *2015)*; *Larsen et al. (2015* [S]*)*; *Manchester, Grímsson & Zetter (2015*[P]*)*	*Oschkinis & Gregor (1992*[P/S]*)*; *Gregor (2005*[P]*)*; *Hottenrott, Gregor & Oschkinis (2010* [P]*)*; *Gregor & Oschkinis (2013* [P]*)*; *Manchester, Grímsson & Zetter (2015*[P]*)*	*Krutzsch & Lenk (1973*[P/S]*)*; *Pälchen & Walter (2011*[S]*)*; *Manchester, Grímsson & Zetter (2015*[P]*)*	*Guo (1979*[P]*)*; *Lei et al. (1992*[P]*)*; *Jin et al. (2002* [P]*)*; *Yao et al. (2009*[P]*)*; *Spicer et al. (2014*[S/P]*)*	*Hochuli (1978*[P]*)*; *Weber & Weiss (1983*[S]*)*; *Eschig (1992*[P/S]*)*; *Grímsson, Ferguson & Zetter (2012*[P]*)*	*Engelhardt (1870* [P]*)*; *Mai & Walther (1991* [P]*)*; *Standke (2008*[S]*)*; *Kmenta (2011* [P]*)*; *Kmenta & Zetter (2013*[P]*)*

Note:
* Following *Cohen et al. (2013*, update*)*.

the collection of the Department of Palaeontology, University of Vienna, Austria, under accession numbers IPUW 7513/076-100.

Molecular framework

For molecular data we relied on a 2014 NCBI GenBank harvest compiled for an earlier study (*Grímsson, Grimm & Zetter, 2017*). Gene banks now (as of December 1st, 2016) include ~100 additional accessions (File S2); but the majority of these are either microsatellite marker sequences or sequences of gene regions too variable, or with insufficient taxonomic coverage within the Loranthaceae, to be of any use; thus, we opted against updating the dataset harvested for the preceding study. All analysis files (sorted by steps) are included in the online supporting archive (OSA) in the Supplementary Information (File S1: Steps 1–3 of analysis pipeline).

Given the problems with signals in Loranthaceae sequence data (*Grímsson, Grimm & Zetter, 2017*: Files S1, S6), we used the following protocol to prepare data sets for phylogenetic inferences and molecular dating (a detailed description is provided in File S1). First, we performed single-gene maximum likelihood (ML) inferences for five candidate gene regions using the complete harvested data with RAxML v. 8.2.4 (*Stamatakis, 2014*). This was mainly done to cross-check for problematic accessions and to test the phylogenetic coherence of multiple accessions of the same species/genus. As a consequence, we eliminated several more sequences, in addition to the ones not considered earlier, for computing strict genus-consensus sequences (see File S1, an emended version of *Grímsson, Grimm & Zetter, 2017*: File S2). The second step was to consense and concatenate the unproblematic data: strict species-consensus sequences, i.e. sequences summarising the information of accessions attributed to a species, were computed with G2CEF (*Göker & Grimm, 2008*) and concatenated with MESQUITE v. 2.75 (*Maddison & Maddison, 2011*). The third and final step was the inference of single- and oligo-gene ML trees using RAxML; branch support was established using non-parametric bootstrapping with the number of necessary bootstrap replicates determined by the extended majority rule consensus bootstop criterion (*Pattengale et al., 2009*). Potentially conflicting signals were explored using bootstrap (BS) consensus networks (bipartition networks; *Grimm et al., 2006*), a special form of consensus networks (*Holland & Moulton, 2003*) generated with SPLITSTREE v. 14.2 (option 'count', *Huson & Bryant, 2006*) in which edge lengths are proportional to the frequency of the according split in the BS (pseudo)replicate sample. The complex signal and overall divergence in the molecular data calls for a probabilistic inference method (i.e. ML or Bayesian inference), and a means for establishing branch support that can reflect the robustness of (partly) conflicting signals from the data. Regarding the latter, non-parametric bootstrapping is more informative (conservative) than Bayesian-inferred posterior probabilities (PP). If a certain proportion of alignment patterns (e.g. 30%) support a split B that is in conflict with the dominant split A (supported by 70% of the alignment patterns), the BS support under ML (BS_{ML}) will be accordingly split in the optimal case (BS_{ML} ~70 for A vs. BS_{ML} ~30 for B). The PP may converge to 1 for A and 0 for B as the MCMC chain(s) optimise(s) towards the topology that best explains the complete data. For the example of

Loranthaceae, it can be demonstrated that branches with PP ~ 1 >> BS_{ML} in the tree of *Su et al. (2015)* relate to relationships supported only by one gene region (*mat*K), which outcompetes conflicting, partly unambiguous signals from all other gene regions; the latter captured in the BS pseudoreplicate samples (*Grímsson, Grimm & Zetter, 2017*: File S6). Readers interested in the behaviour of PP in comparison to the BS_{ML} support values used here can find the according information in the Supporting Information (File S1: set-up, File S5: results; Bayesian sampled topology files are included in the OSA).

Clock-rooting

A recent re-analysis of available molecular data using genus-consensus sequences (*Grímsson, Grimm & Zetter, 2017*) failed to unambiguously resolve basal relationships in Loranthaceae as was the case in earlier studies using placeholder accessions (*Wilson & Calvin, 2006*; *Vidal-Russell & Nickrent, 2008a*; *Su et al., 2015*; see *Grímsson, Grimm & Zetter, 2017*: File S6, for a critical assessment of the Loranthaceae data included by Su et al.). The problem of topological ambiguity worsens for the species tree inferred here, in part due to data gaps (see Inferences and supplement to *Grímsson, Grimm & Zetter, 2017*). Due to issues regarding ambiguity of the deepest splits within the Loranthaceae and likely outgroup–ingroup long-branch attraction (*Grímsson, Grimm & Zetter, 2017*: File S6), we inferred an alternative, clock-based root (*Huelsenbeck, Bollback & Levine, 2002*) for the Loranthaceae tree using BEAST v. 1.8.2 (*Drummond & Rambaut, 2007*; *Drummond et al., 2012*), following the example of an earlier study on *Acer* (*Renner et al., 2008*). Clock-rooting was performed for five main datasets differing in the gene region coverage (all gene regions, all but excluding the most variable *trn*L intron, 5' exon (can be incomplete) and *trn*L–*trn*F spacer (trnL/LF) region, only plastid regions including or excluding the trnL/LF, only nuclear regions). In addition, the taxon-reduced data set used for the final dating step was analysed (for further details see File S1). For each of the matrices we performed a BEAST run under partition specific substitution models, unconstrained tree topology, a Yule tree prior, and uncorrelated log-normal clock prior [ucld.mean ~ Gamma (0.001, 1,000)]. The best fitting substitution models per partition, among the available in BEAST, were selected with JMODELTEST (*Darriba et al., 2012*). Each analysis was conducted for 2×10^7 generations with a sampling frequency of 10^{-3} (for further details see File S1) (Table 2; Step 4 of analysis pipeline).

Basic setup of molecular dating

Nine of the 13 new described fossil pollen from the Eocene to Oligocene (see Results) were used as minimum age constraints (informing three to five node height priors per analysis) for traditional node dating using a Bayesian uncorrelated clock (UC) approach; analyses were performed with BEAST v. 1.8.2. Table 2 lists the age priors used for the analyses. Dating was done in two phases (for set-up details see File S1). With respect to the non-trivial matrix signals and the branch-lengths seen in the ML tree, rate shifts should be considered during dating. Hence, we chose to use the UC approach over other node-dating alternatives (e.g. *Renner et al., 2008*; *Smith, Beaulieu & Donoghue, 2009*; see e.g. *Dornburg et al., 2012* for bias in the case of mammal mtDNA) (Table 2; Steps 5 and 6 of analysis pipeline).

Table 2 Results of the clock-rooting analyses.

Species set	Gene set	Inferred root
All	All	Between Lorantheae core clade and all other Loranthaceae (including Loranthinae and Ileostylinae; not used as rooting scenario for subsequent analyses)
All	All, excluding trnL/LF	Between Lorantheae and all other Loranthaceae (= rooting scenario 2)
All	Nuclear ribosomal DNAs only	Between Lorantheae and all other Loranthaceae (= rooting scenario 2)
All	Chloroplast regions only	Between Lorantheae and all other Loranthaceae (= rooting scenario 2)
All	Chloroplast genes only	Between Lorantheae and all other Loranthaceae (= rooting scenario 2)
Reduced	All	Between *Nuytsia* and all other Loranthaceae (equals outgroup inferred root; = rooting scenario 1)

In the initial phase (Step 5), we inferred dated species phylogenies based on the complete concatenated data set for three rooting scenarios: (1) the commonly accepted root placing *Nuytsia* as sister to all other Loranthaceae (*Vidal-Russell & Nickrent, 2008a*; *Nickrent et al., 2010*; *Su et al., 2015*); (2) a clock-inferred root recognising the predominately Old World Lorantheae as sister to a mainly southern hemispheric clade that includes all three root parasites, the Psittacantheae and Elytrantheae (see Results); and (3) recognising *Tupeia* as sister to all other Loranthaceae. The 3rd scenario is based on the hypothesis that the typical oblate, ± triangular Loranthaceae pollen (Pollen Type B in *Grímsson, Grimm & Zetter, 2017*, a pollen type unique within the Santalales) evolved only once. The monotypic *Tupeia* is one of two Loranthaceae species with a spheroidal, echinate pollen as found in other Santalales lineages (*Grímsson, Grimm & Zetter, 2017*) and the only one sequenced so far. Irrespective of the data used, *Tupeia* is the taxon with the smallest root-tip distance within Loranthaceae, including trees rooted with *Nuytsia* (*Su et al., 2015*: Fig. 1B; *Grímsson, Grimm & Zetter, 2017*; this study).

For the final dating (Step 6), we used a taxon-reduced data set limited to 42 species covering all included gene regions to counter problems with missing data in the full data set. At this step we also included an alternative topology, which constrained the primary branching patterns seen in the tree of *Su et al. (2015)*. This alternative topology was suggested by an anonymous reviewer reporting on the draft to *Grímsson, Grimm & Zetter (2017)* to depict the correct relationships between the major lineages and potentially early diverging, isolated, monotypic genera. Each analysis ran for 5×10^7 MCMC steps, under a similar set-up as described in the preceding step (*clock-rooting*). The tree was partially constrained each time to accommodate the placement of the fossils and the corresponding rooting hypothesis (see xml-setup files provided in the supplemental information [OSM], for details). Each analysis was run twice to ensure the runs converged to the stationary distribution. Finally, all age calibration priors (Table S1-1 in File S1) were modelled as normal distributions around the midpoint of the known time intervals (for further details see File S1). With respect to the variations in plant evolutionary rates (e.g. *Guzmán & Vargas, 2010*; *Lockwood et al., 2013*), we opted against performing any rate-based dating. *Smith & Donoghue (2008)* cautioned against the use of rate-based estimates of divergence times even when fossil calibration priors are lacking as it may lead to strong biases.

DESCRIPTIONS

Some lineages (tribes, subtribes) and genera of modern Loranthaceae are characterised by unique pollen morphologies (autapomorphies in a strict Hennigian sense) or specific pollen character suites (*Grímsson, Grimm & Zetter, 2017*). Nevertheless, we refrained from using genus names to address the fossil pollen types described here—even if the pollen was highly similar or indistinguishable from a modern counterpart—for several reasons: (1) intra- and interspecific variation is not comprehensively understood in Loranthaceae; (2) the generic concepts in Loranthaceae are under on-going revision, (3) monotypic modern lineages/genera could have been more widespread and diverse in the past; and (4) occurrence of fossils combining features of two or more genera or lineages. Thus, all pollen grains are classified as morphotypes (MT) named after the locality where they were found (Figs. 1–6).

All fossil pollen described here falls within the variation of Pollen Type B according *Grímsson, Grimm & Zetter (2017)*. Pollen grains of Type B are oblate (to various degrees), triangular to trilobate in polar view and show a ± psilate sculpturing in LM. They are basically syn(3)colpate, but also demisyn(3)colpate and zono(3)colpate (terminology follows *Punt et al., 2007*; see *Grímsson, Grimm & Zetter, 2017*: Fig. 1, for schematic drawings) in some genera/lineages. Usually, no further sculpturing details can be observed in LM except for occasional exine thickening or thinning at the pole (e.g. Figs. 1C, 1H, 1M, 1Y) and along the colpi or in the mesocolpium (e.g. Figs. 1C, 1D, 1R).

Miller Clay Pit MT1, aff. *Nuytsia*

Description

Pollen, oblate, concave triangular in polar view, no undistorted equatorial view available, equatorial apices obcordate, interapertural areas (mesocolpia) sunken; pollen small, equatorial diameter 15.0–18.3 μm in LM, 13.0–14.4 μm in SEM; zono(3)colpate, colpi long and narrow; exine 0.7–0.8 μm thick, nexine thinner than sexine; tectate; sculpturing psilate in LM, microechinate in area of mesocolpium in SEM, echini 0.3–0.8 μm long, 0.2–0.5 μm wide at base SEM; margo well developed, broad, psilate to partly granulate SEM; colpus membrane not observed (Figs. 1A, 1B, 2A, 2H; Plate S01, S02 in File S3).

Locality

Miller Clay Pit, Henry County, Tennessee, USA (Table 1).

Remarks

This pollen type is very similar to pollen of the extant southwestern Australian *Nuytsia floribunda* (Labill.) G. Don as figured by *Feuer & Kuijt (1980)* and *Grímsson, Grimm & Zetter (2017)*; a pollen readily distinct from all other modern Loranthaceae. The fossil pollen only differs from *Nuytsia* by being zonocolpate and showing sunken (infolded) mesocolpia in LM and SEM. The shift from the basic syncolpate organisation to zonocolpate can be observed in several lineages of (modern) Loranthaceae. With respect to the high genetic distinctness of *Nuytsia* from all other Loranthaceae, the

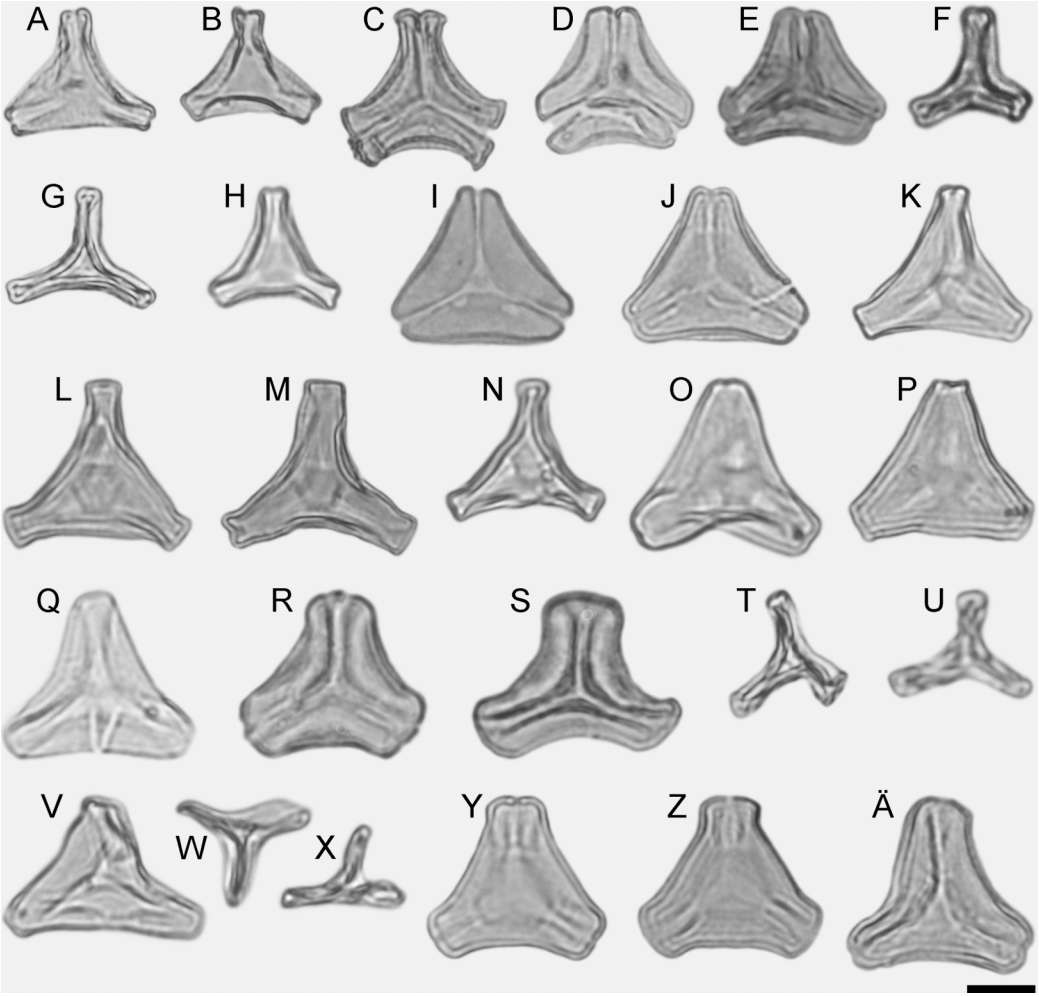

Figure 1 LM micrographs (polar views) of all fossil Loranthaceae morphotypes. (A) Miller Clay Pit MT1. (B) Miller Clay Pit MT1. (C) Miller Clay Pit MT2. (D) Miller Clay Pit MT3. (E) Aamarutissaa MT. (F) Stolzenbach MT. (G, H) Profen MT1. (I, J) Profen MT2. (K) Profen MT3. (L–O) Profen MT4. (P, Q) Profen MT5. (R, S) Changchang MT. (T–X) Theiss MT. (Y–Ä) Altmittweida MT.

modern species likely represents the sole survivor of an early diverged lineage of root parasitic loranths. Hence, it is likely that ancestral or extinct members of *Nuytsia*/Nuytsieae had more morphological variation than can be observed in the sole surviving species.

Use as age constraint

The Miller Clay Pit MT1 can be used to constrain the root age of the lineage leading to *Nuytsia*, i.e. the Nuytsieae root age. Based on the currently available molecular data, the relationship of *Nuytsia* to the remainder of the genus and the other two extant root parasites is unclear. Nevertheless, *Nuytsia* is likely the sole modern-day representative of an early diverging lineage. For rooting scenario 1 (outgroup-inferred root) Miller Clay Pit MT1 serves as minimum age constraint for the MRCA of all (extant) Loranthaceae.

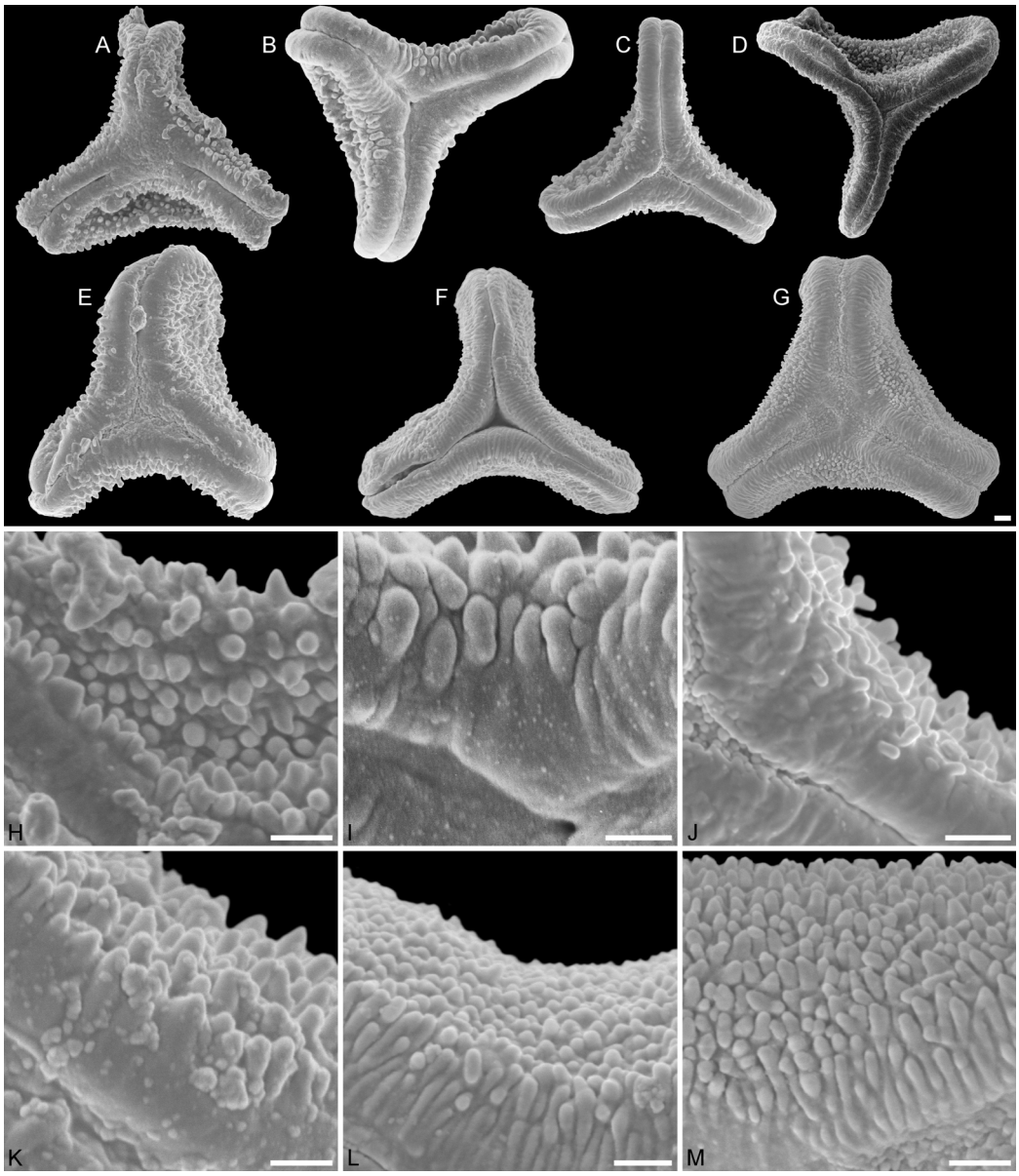

Figure 2 SEM micrographs of fossil Loranthaceae pollen similar to/intermediate between root parasites and Lorantheae and comparable extant pollen. (A–D) Polar views of fossil pollen. (E–G) Polar views of extant pollen. (H–J) Close-ups of sculpturing in area of mesocolpium and along margo in fossil pollen. (K–M) Close-ups of sculpturing in area of mesocolpium and along margo in extant pollen. (A, H) Miller Clay Pit MT1. (B, I) Stolzenbach MT. (C, J) Profen MT1. (D) Theiss MT. (E, K) *Nuytsia floribunda*. (F, L) *Gaiadendron punctatum*. (G, M) *Muellerina eucalyptoides*. Scale bars: (A–M) = 1 μm.

Miller Clay Pit MT2, aff. *Tripodanthus*

Description

Pollen, oblate, concave-triangular in polar view, no undistorted equatorial view available, equatorial apices T-shaped; pollen small, equatorial diameter 18.3–21.7 μm in LM, 17.9–20.2 μm in SEM; syn(3)colpate, colpi narrow; exine 1.2–1.5 μm thick, nexine thinner than sexine, intercolpial nexine thickening at pole, sexine thickened in area of

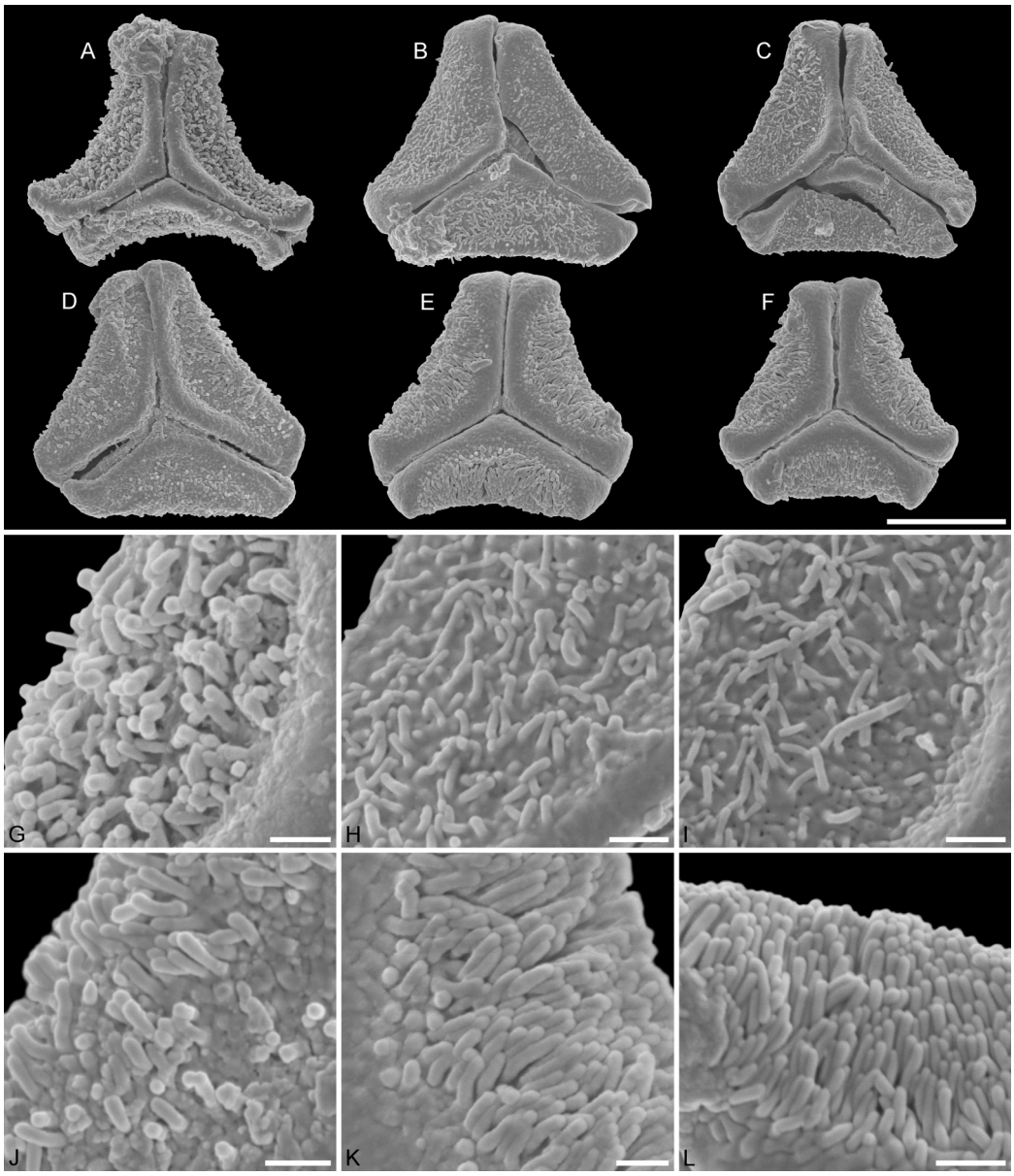

Figure 3 SEM micrographs of fossil Loranthaceae pollen with affinity to *Tripodanthus* and extant pollen of the genus. (A–D) Polar views of fossil pollen. (E, F) Polar views of extant pollen. (G–J) Close-ups of sculpturing in area of mesocolpium and along margo in fossil pollen. (K, L) Close-ups of sculpturing in area of mesocolpium and along margo in extant pollen. (A, G) Miller Clay Pit MT2. (B, C, H, I) Miller Clay Pit MT3. (D, J) Aamaruutissaa MT. (E, F, K, L) *Tripodanthus acutifolius*. Scale bars: (A–F) = 10 μm, (G–L) = 1 μm.

mesocolpium (LM); tectate; sculpturing psilate in LM, (micro)baculate in area of mesocolpium in SEM, (micro)bacula densely packet, 0.2–0.9 μm long, 0.2–0.4 μm wide SEM; margo well-developed, widening towards pole and equator, mostly psilate, with few nanoechini/-verrucae SEM; colpus membrane not observed (Figs. 1C, 3A, 3G; Plate S03 in File S3).

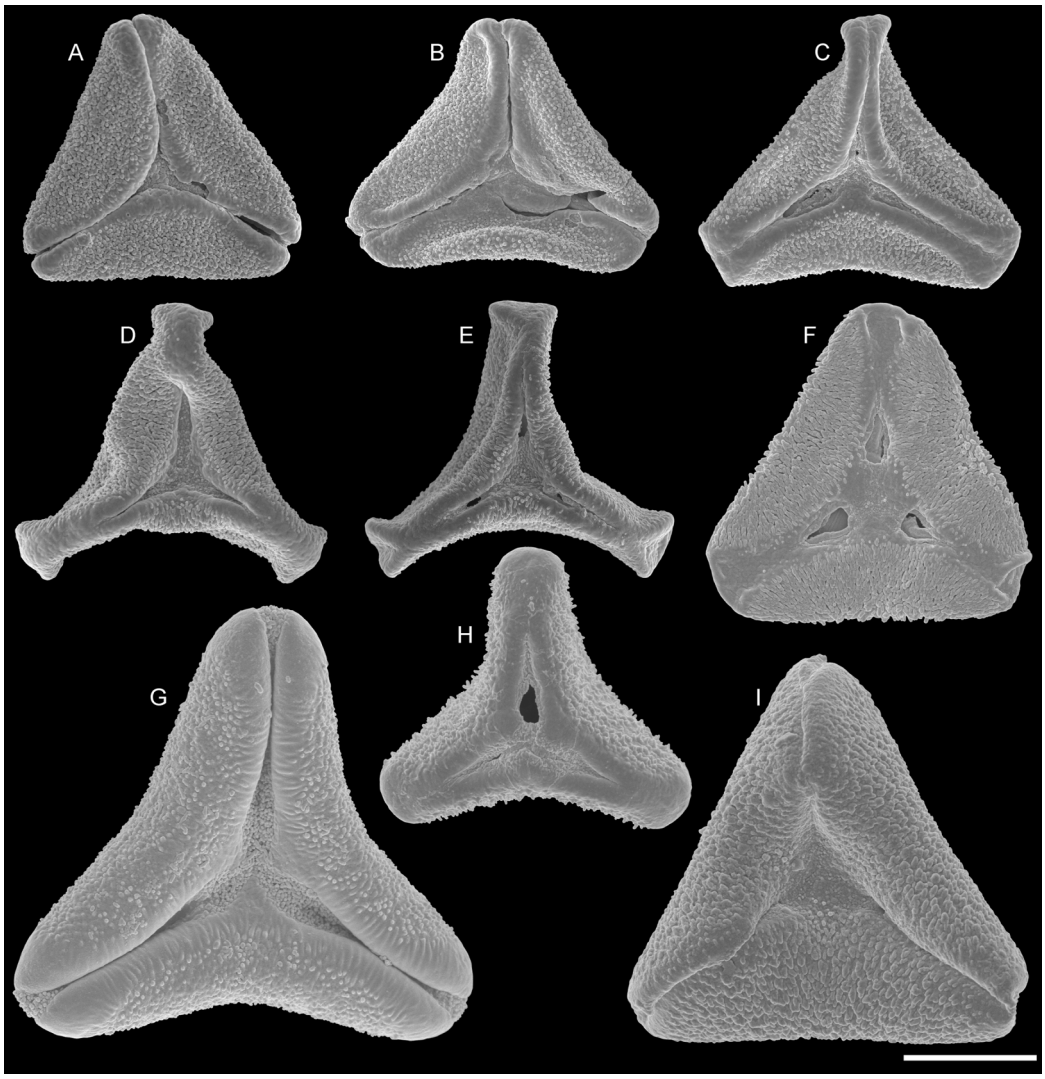

Figure 4 SEM micrographs of fossil Loranthaceae pollen with affinity to Elytrantheae and extant representatives. (A–F) Polar views of fossil pollen. (G–I) Polar views of extant pollen. (A, B) Profen MT2. (C) Profen MT3. (D, E) Profen MT4. (F). Profen MT5. (G) *Peraxilla tetrapetala*. (H) *Amylotheca* sp. (I) *Ligaria cuneifolia*. Scale bar: (A–I) = 10 μm.

Locality

Miller Clay Pit, Henry County, Tennessee, USA (Table 1).

Remarks

Pollen grains of this morphotype show the exclusive morphology of pollen of two of the three extant *Tripodanthus* species: *Tripodanthus acutifolius* (Ruiz & Pav.) Tiegh. and *Tripodanthus flagellaris* Tiegh. as described and figured by *Feuer & Kuijt (1980)* and *Grímsson, Grimm & Zetter (2017)*. The recently described *Tripodanthus belmirensis* F. J. Roldán & Kuijt has a different, more compact type of pollen (*Roldán & Kuijt, 2005*). All species are endemic to South America (e.g. *Amico et al., 2012*).

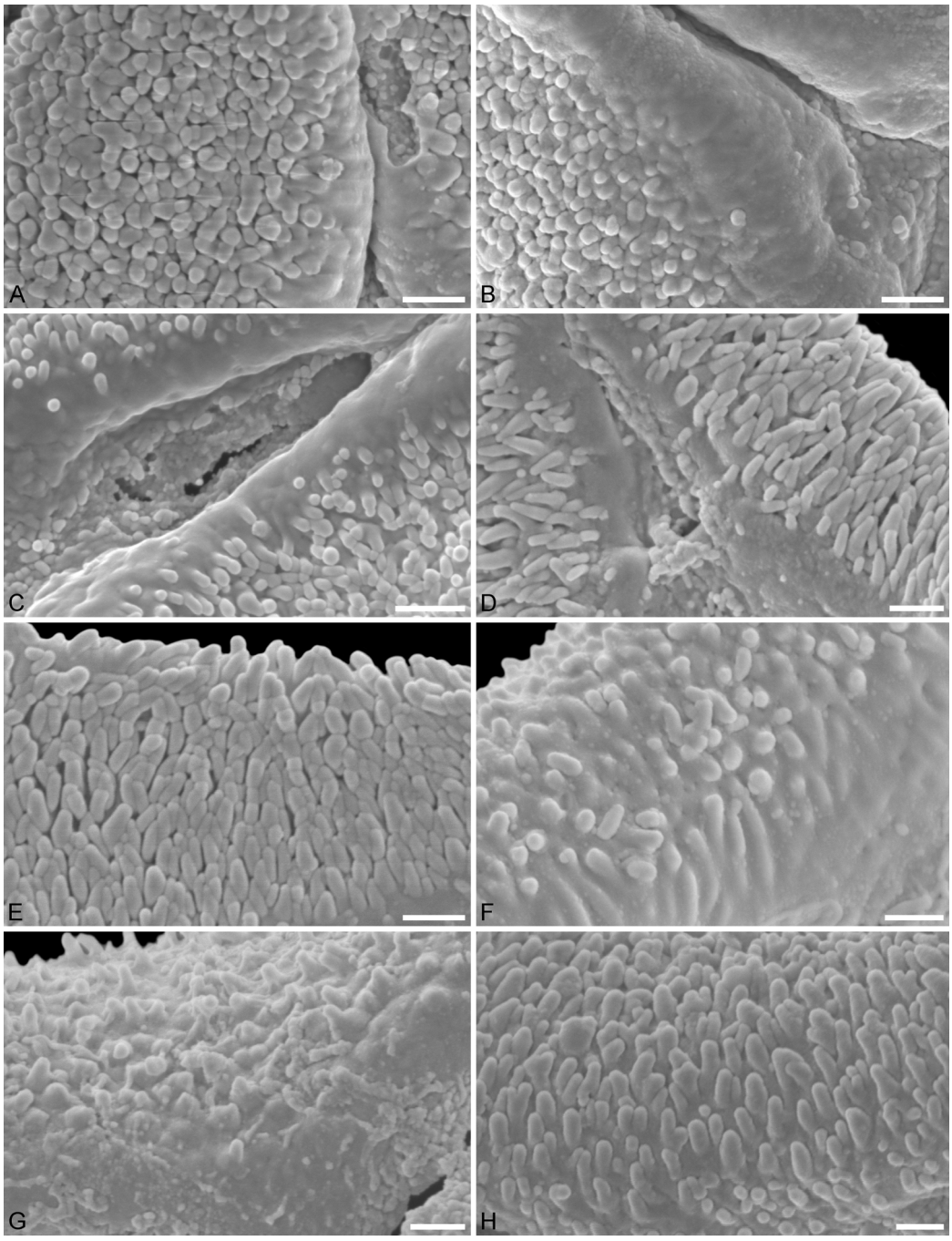

Figure 5 SEM micrographs of fossil Loranthaceae pollen with affinity to Elytrantheae and extant representatives. (A–E) Close-ups of sculpturing in area of mesocolpium and along margo in fossil pollen. (F–H) Close-ups of sculpturing in area of mesocolpium and along margo in extant pollen. (A, B) Profen MT2. (C) Profen MT3. (D) Profen MT4. (E) Profen MT5. (F) *Peraxilla tetrapetala*. (G) *Amylotheca* sp. (H) *Ligaria cuneifolia*. Scale bar: (A–H) = 1 μm.

Use as age constraint

Representing a characteristic pollen type known only from two modern species of the same genus, Miller Clay Pit MT2, MT3, and the Aamaruutissaa MT could be used as

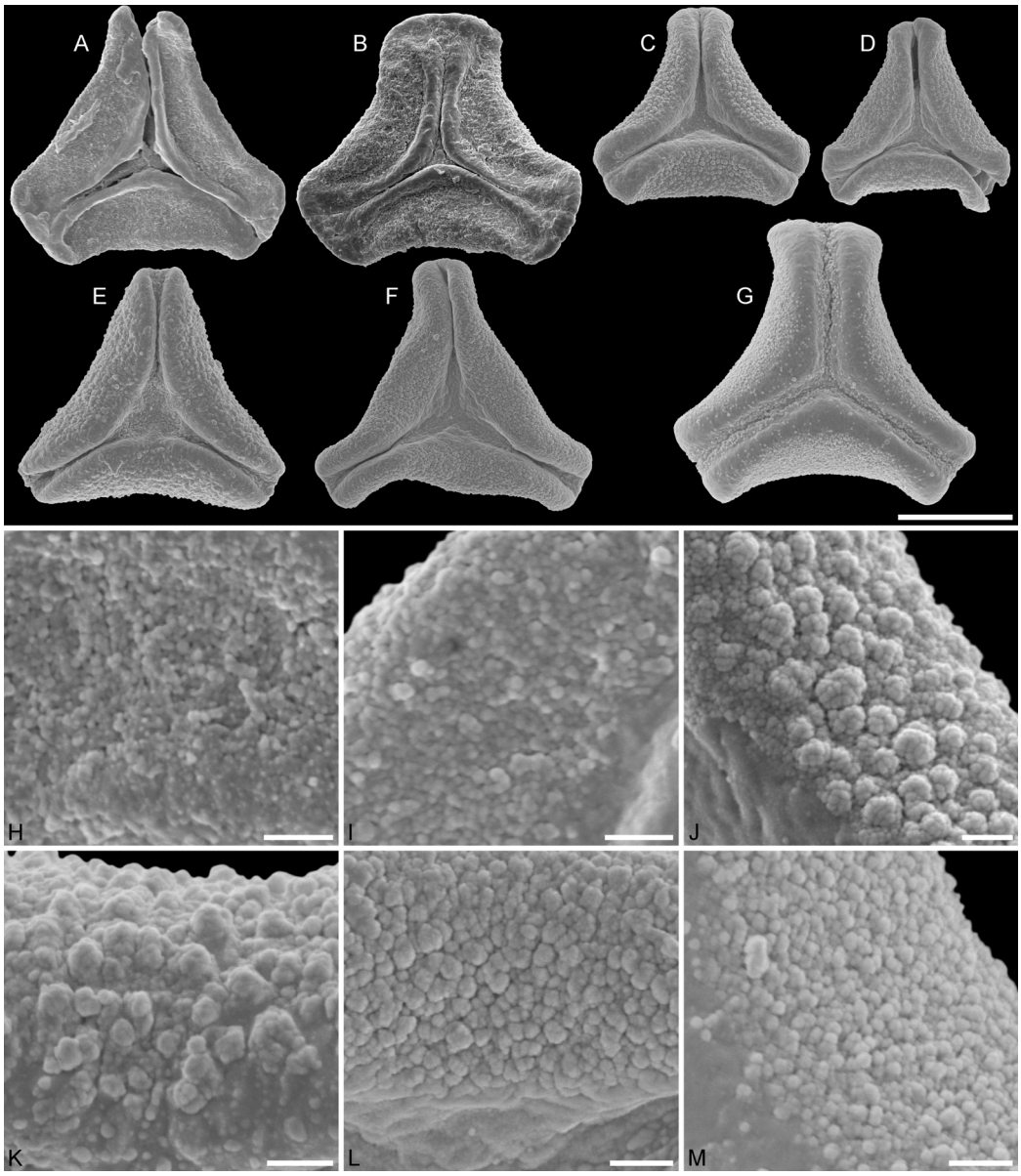

Figure 6 SEM micrographs of fossil Loranthaceae pollen with affinity to crown group Lorantheae and comparable extant pollen. (A–D) Polar views of fossil pollen. (E–G) Polar views of extant pollen. (H–J) Close-ups of sculpturing in area of mesocolpium and along margo in fossil pollen. (K–M) Close-ups of sculpturing in area of mesocolpium and along margo in extant pollen. (A, B, H, I) Changchang MT. (C, D, J) Altmittweida MT. (E, K) *Amyema gibberula*. (F, L) *Helixanthera kirkii*. (G, M) *Taxillus caloreas*. Scale bars: (A–G) = 10 μm, (H–M) = 1 μm.

minimum age constraints for the MRCA of *Tripodanthus* with respect to *Tripodanthus belmirensis* and its different pollen. We followed a more conservative approach here. *Tripodanthus* is often reconstructed as the first diverging branch within the Psittacanthinae, followed in most trees by *Psittacanthus*. The latter is a genus with diverse pollen (*Feuer & Kuijt, 1979*), including morphologies more similar to those of *Tripodanthus* and its fossil counterparts than to the remainder of the subtribe

(and *Tripodanthus belmirensis*). The remainder is characterised by compact B-type pollen with minute to indistinct sculpturing and pollen grains of the Type C (*Passovia pyrifolia, Dendropemon*) and D (*Oryctanthus*). Compact B-type, C-type and D-type pollen occur much later in the fossil record (File S4) and are completely missing in our samples. The latter three types appear to be derived. Taking all evidence into account, we cannot exclude the possibility that *Tripodanthus acutifolius* and *Tripodanthus flagellaris* simply retained a more ancestral pollen type of the Psittacanthinae. The fossil pollen grains hence would not indicate the presence of the genus *Tripodanthus* in North America and Greenland, but of extinct, northern-hemispheric or ancestral members of the Psittacanthinae, thereby informing a conservative minimum age for the MRCA of Psittacanthinae and their sister clade. Unfortunately, this sister clade, if not constrained (scenario 4), is not resolved with meaningful support. As a trade-off, we used the Aamaruutissaa MT—the most precisely dated pollen of the *Tripodanthus*-like MTs and likely younger than their American counterparts—as minimum age constraint for the MRCA of the Psittacanthinae lineage for the rooting scenarios 1–3 (under the assumption that crown radiation within the Psittacanthinae must have started before the time of a loranth that produced *Tripodanthus*-like pollen and thrived in Greenland, far outside the modern distribution area of the family.)

Miller Clay Pit MT3, aff. *Tripodanthus*

Description

Pollen, oblate, slightly concave-triangular in polar view, no undistorted equatorial view available, equatorial apices truncated; pollen small, equatorial diameter 20.0–21.7 μm in LM, 19.6–21.3 μm in SEM; syn(3)colpate, colpi narrow; exine 0.9–1.6 μm thick, nexine thinner than sexine, intercolpial nexine thickening at pole, sexine thickened in area of mesocolpium (LM); tectate; sculpturing psilate in LM, (micro)baculate and perforate in area of mesocolpium in SEM, (micro)bacula densely packet, (micro)bacula 0.4–1.8 μm long, 0.1–0.2 μm wide; margo well developed, markedly broader in equatorial regions, margo faintly nano- to micro-rugulate SEM; colpus membrane nanoverrucate to granulate SEM (Figs. 1D, 3B, 3C, 3H, 3I; Plate S04 in File S3).

Locality

Miller Clay Pit, Henry County, Tennessee, USA (Table 1).

Remarks

General outline and size of the Miller Clay Pit MT3 is very similar to those of Miller Clay Pit MT2. The main difference is that the margo in Miller Clay Pit MT3 can be faintly rugulate, a feature not observed in Miller Clay Pit MT2 or the two extant species with nearly identical pollen. Also, the mesocolpium is perforate in Miller Clay Pit MT3; a feature not seen in Miller Clay Pit MT2 or extant *Tripodanthus*. As a trend, the sculptural elements are narrower and can be much longer than in Miller Clay Pit MT2 pollen.

Use as age constraint

See Miller Clay Pit MT2.

Aamaruutissaa MT, aff. *Tripodanthus*

Description

Pollen, oblate, slightly concave-triangular in polar view, no undistorted equatorial view available, equatorial apices truncated; pollen small, equatorial diameter 18.6–22.0 μm in LM, 18.5–21.5 μm in SEM; syn(3)colpate; exine 1.0–1.3 μm thick, nexine thinner than sexine, intercolpial nexine thickening at pole (LM); tectate; sculpturing psilate in LM, nano- to microbaculate in area of mesocolpium in SEM, bacula 0.3–1.1 μm long, 0.2–0.3 μm wide SEM; margo well developed, margo faintly nano- to microrugulate SEM; colpus membrane nanoverrucate to granulate SEM (Figs. 1E, 3D, 3J; Plate S05 in File S3).

Locality

Aamaruutissaa, southeast Qeqertarsuatsiaq Island, western Greenland (Table 1).

Remarks

This pollen type has previously been figured as Loranthaceae gen. et spec. indet. (*Manchester, Grímsson & Zetter, 2015*: Figs. 2A–2C). Like Miller Clay Pit MT2 and MT3, it is nearly indistinguishable from the pollen of the two original species of *Tripodanthus, Tripodanthus acutifolius* and *Tripodanthus flagellaris.* The Aamaruutissaa MT pollen combines the mesocolpial sculpturing seen in Miller Clay Pit MT2 with the shape and margo seen in Miller Clay Pit MT3. With respect to the modern species, both the Tennessee (Miller Clay Pit MT2, MT3) and Greenland pollen grains (Aamaruutissaa MT) were possibly produced by the same genus or at least closely related taxa of the same loranth lineage (Psittacanthinae).

Use as age constraint

See Miller Clay Pit MT2.

Stolzenbach MT, pollen of ambiguous affinity

Description

Pollen, oblate, trilobate in polar view, no undistorted equatorial view available, equatorial apices obcordate, interapertural areas (mesocolpia) sunken; pollen small, equatorial diameter 12.1–15.4 μm in LM, 11.7–15.3 μm in SEM; syn(3)colpate, colpi narrow; exine 0.7–0.9 μm thick, nexine thinner than sexine; tectate; sculpturing psilate in LM, microechinate in area of mesocolpium in SEM, echini stout with blunt apices, 0.4–0.8 μm long, 0.3–0.8 μm wide at base SEM; margo well developed, broad, covering the grain's surface in polar view, microrugulate, granulate SEM; colpus membrane mostly granulate SEM (Figs. 1F, 2B, 2I; Plate S06 in File S3).

Locality

Stolzenbach underground coalmine, Kassel, Germany (Table 1).

Remarks

Size, outline, and form of the pollen, and SEM sculpturing in the area of the mesocolpium is most similar to what has been observed in pollen of modern monotypic root-parasites *Nuytsia* and *Gaiadendron*, and the Lorantheae *Muellerina* (Ileostylinae). Despite this

general similarity, the pollen differs from the modern ones and pollen with affinity to *Nuytsia* reported from the Miller Clay Pit, Tennessee (Miller Clay Pit MT1), visually (compare overviews in Figs. 2B, 2E, 2F, 2G) and regarding its sculpturing. The Stolzenbach MT echini are sparsely packed and broader at the base; the striae on the margo are flatter and broader. The pollen may well represent an unrelated, extinct lineage or ancestral taxon with affinities to both the root-parasitic lineages and/or the Lorantheae.

Use as age constraint

Although the pollen cannot be assigned to any modern genus or lineage, it is an early Central European representative of the common Pollen Type B of Loranthaceae. Its morphology is in many aspects primitive within the (B-type) Loranthaceae, hence, the similarity with *Nuytsia*/Miller Clay Pit MT1, *Gaiadendron*, and *Muellerina* (the only Lorantheae known so far with a striate ornamentation). Its morphology, place, and age would fit for an early precursor or extinct sister lineage of the Lorantheae. Taken together with the coeval pollen from North America and Greenland, it provides evidence for the onset of diversification of B-type pollen lineages including the possible establishment of the Lorantheae. Hence, it was used to constrain the minimum age of the MRCA of all Loranthaceae (rooting scenario 2; clock-based root) or Loranthaceae with B-type pollen (rooting scenario 3; pollen morphology-informed root).

Profen MT1, pollen of unknown affinity

Description

Pollen, oblate, trilobate in polar view, elliptic in equatorial view, lobes very narrow, equatorial apices obcordate, interapertural areas (mesocolpia) sunken; pollen small, polar axis 10.0–12.3 μm long in LM, 9.5–11.0 μm long in SEM, equatorial diameter 13.8–17.5 μm in LM, 11.9–13.8 μm in SEM; syn(3)colpate; exine 0.9–1.1 μm thick, nexine thinner than sexine; tectate; sculpturing psilate in LM, nanoechinate, nanobaculate, granulate in area of mesocolpium in SEM, echini/bacula 0.3–0.6 mm long, 0.2–0.4 μm wide SEM; margo well-developed, covering nearly the entire surface of the grain in polar view, faintly microrugulate SEM; colpus membrane nanoverrucate to granulate SEM (Figs. 1G, 1H, 2C, 2J; Plate S07 in File S3).

Locality

Profen, Leipzig, Central Germany (Table 1).

Remarks

Like the Stolzenbach MT pollen this fossil pollen type has no direct modern counterpart. These small, narrow-lobate pollen grains with their finely sculptured, deeply sunken mesocolpia characteristic of the Profen MT1 pollen are not found in any modern taxon, but bear some similarity to the younger (Oligocene) pollen of Theiss (see below). Equally small pollen grains are only known from the root-parasites *Nuytsia* and *Gaiadendron*, and the Lorantheae *Muellerina*. Equally minute sculpturing is only found in otherwise completely different, and putatively derived pollen of deeply nested (phylogenetically) Psittacanthinae and Lorantheae.

Use as age constraint

Showing a unique combination of putatively primitive and derived morphological features, this pollen could only be used to constrain the minimum age of the MRCA of all Loranthaceae with B-type pollen.

Profen MT2, aff. *Notanthera*

Description

Pollen, oblate, straight- to slightly concave-triangular in polar view, no undistorted equatorial view available, equatorial apices obcordate; pollen small, equatorial diameter 21.5–23.1 μm in LM, 18.3–19.6 μm in SEM; syn(3)colpate, colpi narrow; exine 1.1–1.4 μm thick, nexine thinner than sexine, intercolpial nexine thickening at pole, sexine thickened in area of mesocolpium (LM); tectate; sculpturing psilate in LM, nano-echinate/-baculate, perforate in area of mesocolpium in SEM, echini/bacula stout, sometimes fused, 0.2–0.4 μm long, 0.2–0.4 μm wide SEM; margo well-developed, slightly widening towards pole and equator, psilate to faintly microrugulate SEM; colpus membrane nanoverrucate to granulate SEM (Figs. 1I, 1J, 4A, 4B, 5A, 5B; Plate S08 in File S3).

Locality

Profen, Leipzig, Central Germany (Table 1).

Remarks

Form and sculpturing of pollen grains of this morphotype are remarkably similar to those of *Notanthera heterophylla* (*Feuer & Kuijt, 1980*: Fig. 5). *Notanthera heterophylla* is one of two species that comprise the two monotypic genera of the South American Notantherinae; a subtribe of the Psittacantheae neither resolved as clade nor rejected with high support in molecular-phylogenetic inferences (*Grímsson, Grimm & Zetter, 2017*: Files S1, S6). The sculpturing of Profen MT2 is furthermore in line with the description and TEM image provided by *Feuer & Kuijt (1980)*.

Systematic note

The second species included in the Notantherinae, *Desmaria mutabilis* (Poepp. & Endl.) Tiegh. ex B.D.Jacks., has not only a different pollen (*Feuer & Kuijt, 1980*; *Grímsson, Grimm & Zetter, 2017*) but is also genetically distinct (Fig. 7).

Use as age constraint

This pollen can inform the minimum root age for the lineage leading to *Notanthera*, i.e. the minimum age of the MRCA of *Notanthera* and Elytrantheae (scenarios 1–3; preferred topology based on the taxon-reduced data set) or *Notanthera* and Psittacanthinae (scenario 4; topology constrained to fit with *Su et al., 2015*: Fig. 1B).

Profen MT3, pollen of the Elytrantheae clade

Description

Pollen, oblate, convex-triangular in polar view, no undistorted equatorial view available, equatorial apices more or less truncated; pollen small, equatorial diameter 20.0–21.5 μm

in LM, 19.2–20.0 μm in SEM; syn(3)colpate, colpi very narrow at equatorial apices, widening towards the pole; exine 0.9–1.1 μm thick, nexine thinner than sexine (LM); tectate; sculpturing psilate in LM, mostly nano-baculate to -echinate in area of mesocolpium in SEM, bacula/echini 0.2–0.5 μm long, 0.1–0.2 mm wide SEM; margo well developed, covering the equatorial apices, mostly psilate, with few nano-bacula/-echini in polar area, forming triangular protrusions at pole SEM; colpus membrane nano-echinate/-verrucate to granulate SEM (Figs. 1K, 4C, 5C; Plate S09 in File S3).

Locality

Profen, Leipzig, Central Germany (Table 1).

Remarks

The combination of characters (syncolpate with widening colpi, margo with triangular protrusions and sculpturing reminiscent of the mesocolpium in polar area, sculpturing of mesocolpium nano-baculate/-echinate) is today only found in members of the Elytrantheae. With respect to studied modern Elytrantheae, the pollen of Profen MT3 resembles the most that of *Peraxilla tetrapetala* (L.f.) Tiegh. (Fig. 4), but the sculpturing elements are more slender and higher (Fig. 5). The sculpturing in the mesocolpium (dimension and density of sculptural elements) matches grains included in another morphotype found at Profen (Profen MT4; Fig. 5).

Use as age constraint

Here we used Profen MT3, MT4 and MT5 to constrain the root age of the Elytrantheae, i.e. the minimum age of the MRCA of *Notanthera* and Elytrantheae (scenarios 1–3). Further studies of modern pollen of Elytrantheae at and below the genus level and more genetic data are needed to decide whether the Profen MT3, and the related Profen MT4 and MT5, are already indicative for a first divergence within the Elytrantheae and can be placed more decisively within the Elytrantheae subtree.

Profen MT4, possible pollen of the Elytrantheae clade

Description

Pollen, oblate, concave-triangular to trilobate in polar view, no undistorted equatorial view available, equatorial apices T-shaped; pollen small, polar axis 11.3–15.0 μm long in LM, equatorial diameter 17.5–25.0 μm in LM, 14.3–20.0 μm in SEM; demisyn(3)colpate, colpi short SEM, widening towards the pole forming a polar depression (polar sexine reduced); exine 1.1–1.3 μm thick, nexine thinner than sexine, nexine hexagonally thickened in polar area (LM); tectate; sculpturing psilate in LM, mostly nano-baculate/-echinate in SEM, bacula/echini 0.3–1.1 μm long, 0.1–0.4 μm wide at base SEM; margo indistinct in polar area, more prominent in equatorial regions, faintly microrugulate, covered by nano-bacula/-echini in polar area SEM; colpus membrane nano-echinate/-verrucate to granulate SEM (Figs. 1L–1O, 4D, 4E, 5D; Plate S10, S11 in File S3).

Locality

Profen, Leipzig, Central Germany (Table 1).

Remarks

This pollen type has previously been figured (*Manchester, Grímsson & Zetter, 2015*: Figs. 2D–2F), designated as "Loranthaceae gen. et spec. indet." Sculpturing of Profen MT4 is somewhat variable; dimensions, density and shape of sculptural elements resemble those in Profen MT3 and Profen MT5 (see later), or are overlapping between both. Regarding its form (trilobate with T-shaped equatorial apices) and lacking a distinct margo in the polar area, the pollen differs from all modern members of the Elytrantheae. In this aspect, it is similar to the pollen of *Ligaria* (Psittacantheae: Ligarinae), a genus with ambiguous phylogenetic affinities to other New World genera (*Grímsson, Grimm & Zetter, 2017*: File S1, Figs. S6-1–9). Also in *Ligaria*, the sexine is reduced in the polar area (Fig. 4), the generally very narrow colpi are fusing in a triangular polar depression (a feature only seen in *Ligaria* and its putative relative *Tristerix*). *Ligaria* pollen grains are furthermore distinctly microbaculate (Fig. 5). Bacula are found in all three Profen morphotypes linked to the Elytrantheae lineage, but are rare or absent in the modern members of this clade.

Use as age constraint

See Profen MT3.

Profen MT5, probable pollen of the Elytrantheae clade

Description

Pollen, oblate, straight-triangular in polar view, elliptic to subrhombic in equatorial view, equatorial apices broadly rounded; pollen small to medium, polar axis 7.5–11.5 μm long in LM, equatorial diameter 21.5–30.0 μm in LM, 18.7–24.4 μm in SEM; demisyn(3) colpate, widening towards pole, terminating halfway between pole and equator SEM; exine 1.1–1.3 μm thick, nexine thinner than sexine (LM); tectate; sculpturing psilate in LM, mostly nano- to micro-baculate/-echinate in area of mesocolpium in SEM, bacula/echini 0.3–0.7 μm long, 0.1–0.3 mm wide at base; margo distinct but not raised, mostly psilate, with few nano-bacula/-echini in polar area, forming triangular protrusions at pole SEM; colpus membrane nano-echinate/-verrucate to granulate SEM (Figs. 1P, 1Q, 4F, 5E; Plate S12 in File S3).

Locality

Profen, Leipzig, Central Germany (Table 1).

Remarks

The pollen fits with the morphotypes seen in modern members of the Elytrantheae, although its combination of characters is unique. Small, demisyncolpate, (sub)rhombic pollen grains are (so far) only known from *Amylotheca*, which differ from the fossil pollen by their outline in polar view (Fig. 4) and sculpturing (Fig. 5). Regarding the latter, Profen MT5 is very similar to grains included in Profen MT3. Both, Profen MT3 and MT5, differ from the third morphotype with possible affinities to Elytrantheae (Profen MT4) by their demisyncolpate grains (Fig. 4). Regarding the mesocolpium, Profen MT5 shows the densest sculptured mesocolpium of all three morphotypes (Fig. 5).

Use as age constraint

See Profen MT3.

Changchang MT, aff. Amyeminae vel Scurrulinae

Description

Pollen, oblate, concave-triangular to broadly trilobate in polar view, no undistorted equatorial view available, equatorial apices broadly rounded; pollen small, equatorial diameter 21.1–24.4 μm in LM, 19.1–21.8 μm in SEM; syn(3)colpate; exine 0.9–1.1 μm thick, nexine thinner than sexine; tectate; sculpturing psilate in LM, nanoverrucate to granulate, perforate in SEM, granula partly fused; margo well developed, psilate, widening towards the equator, usually covering the entire apex SEM; colpus membrane granulate; rhombic structures (opercula) covering equatorial apices SEM (Figs. 1R, 1S, 6A, 6B, 6H, 6I; Plate S13 in File S3).

Locality

Changchang Basin, Jiazi Town, northern Hainan Island (Table 1).

Remarks

The minute sculpturing and its basic form link this pollen to the Lorantheae, in particular to the Scurrulinae *Taxillus* and *Scurrula* (unresolved within Clade J) on one hand, and *Amyema* (Amyeminae; Clade I in *Vidal-Russell & Nickrent, 2008a*, sister clade of Clade J) on the other hand. The pollen could be described as a Scurrulinae pollen with an *Amyema*-like margo. A unique feature not found in any modern Loranthaceae so far are the operculum-like triangular structures of the equatorial apices. Pollen of the two first diverging, long-branched lineages in Lorantheae (Clades G and H in *Vidal-Russell & Nickrent, 2008a*; cf. *Su et al., 2015*: Figs. 1B, S7; *Grímsson, Grimm & Zetter, 2017*: Fig. 2) are markedly distinct. Thus, we think that this pollen belongs to an extinct or ancestral Lorantheae lineage related to the core Lorantheae (= Clades I and J according Vidal-Russell & Nickrent).

Use as age constraint

Based on its morphology, the Changchang MT could already represent an early member of the Lorantheae core clade, i.e. would inform a minimum age of the MRCA of Lorantheae core clade and its sisterclade Ileostylinae. However, some molecular data sets indicate a sister relationship between Ileostylinae and Loranthinae (cf. *Grímsson, Grimm & Zetter, 2017*: Files S1, S6). Furthermore, more information on pollen morphology in Lorantheae would be needed to exclude the possibility that the Changchang MT is correctly recognised as a representative of the Lorantheae core clade. Two of the four genera of the sister lineages of the core Lorantheae (Loranthinae, Ileostylinae) have not yet been studied palynologically and little is known on the other Amyeminae genera, the first diverging branch within the core Lorantheae. Hence, we opted for a more conservative approach and used the Changchang MT to constrain the MRCA of all Lorantheae.

Theiss MT

Description

Pollen, oblate, trilobate in polar view, emarginate in equatorial view, lobes very narrow, equatorial apices rounded; pollen small, polar axis 8.3–11.7 mm long in LM, 6.5–8.3 μm long in SEM, equatorial diameter 10.0–15.0 μm in LM, 10.3–11.8 μm in SEM; demisyn (3)colpate; exine 0.9–1.2 μm thick, nexine thinner than sexine (LM); tectate; sculpturing psilate in LM, nano- to microverrucate in area of mesocolpium in SEM, verrucae often fused, widely spaced, verrucae composed of conglomerate granula SEM; margo well-developed, covering nearly the entire surface of the grain in polar view, faintly microrugulate, granulate SEM; colpus membrane unknown (Figs. 1T–1X, 2D; Plate S14, S15 in File S3).

Locality

Theiss, borehole southeast of Krems, Lower Austria (Table 1).

Remarks

This fossil pollen type has no direct modern counterpart. A unique feature is the widely spaced verrucae in area of mesocolpium. Demisyncolpate grains evolved at least three times in the Loranthaceae: in *Amylotheca* (Elytrantheae), in the *Cladocolea-Struthanthus* lineage and *Passovia* (Psittacanthinae), and *Tapinanthus* (*T. bangwensis* [Engl. & K.Krause] Danser, *T. ogowensis* [Engl.] Danser; Lorantheae core clade). The fossil pollen shares no other features with either Elytrantheae or Psittacanthinae. Grains with narrow (deflated) equatorial lobes, in which the margo extends beyond the mesocolpial plane, are so far only known from several members of the Lorantheae core clade (e.g. *Englerina, Globimetula, Phragmanthera*). Mesocolpia with exclusively nanoverrucate to granulate sculpturing are only found in members of the Lorantheae. For instance, the Tapinanthinae (core Lorantheae) *Actinanthella* has emarginate, trilobate (to convex-triangular) pollen grains with a well-developed, mostly psilate margo and nanoverrucate to granulate mesocolpium, but they differ from the fossil pollen by their size and zonocolpate apertures.

Use as age constraint

Due to the unique morphology, yet superficial knowledge about pollen evolution in Lorantheae (see Changchang MT), we decided against using the Theiss MT to constrain a node higher up in the tree (e.g. the MRCA of Tapinanthinae and Emelianthinae).

Altmittweida MT, aff. *Helixanthera*

Description

Pollen, oblate, convex-triangular in polar view, emarginate in polar view, equatorial apices broadly obcordate; pollen small, polar axis 4.4–5.5 μm long in LM, equatorial diameter 14.4–17.8 μm in LM, 13.7–16.0 μm in SEM; syn(3)colpate; exine 0.9–1.1 μm thick, nexine thinner than sexine, intercolpial nexine thickening at pole, sexine partly reduced in polar area SEM; tectate; sculpturing psilate in LM, nano- to micro-verrucate, granulate in SEM, verrucae composed of conglomerate granula (Fig. 6J); margo psilate to

microverrucate, granulate; colpus membrane nanoverrucate to granulate SEM (Figs. 1Y–1Ä, 6C, 6D, 6J; Plate S16 in File S3).

Locality

Altmittweida, Saxony, Germany (Table 1).

Remarks

This pollen type has previously been figured by *Kmenta (2011*: Plate 11, Figs. 1–3*)* as "Loranthaceae gen. et spec. indet." Pollen very similar to this fossil pollen can be found in two extant species of the Lorantheae: *Amyema gibberula* Danser (type genus of Amyeminae, Clade I according *Vidal-Russell & Nickrent, 2008a*) and *Helixanthera kirkii* (Oliv.) Danser (*Grímsson, Grimm & Zetter, 2017*). Both species are similar in outline (convex-triangular, emarginate) and sculpturing (margo indistinct, with similar sculpturing than adjacent mesocolpium). In LM, *Amyema* shows a distinct hexagonal thickening of the polar nexine, whereas in *Helixanthera* the thickening covers a larger area of the grain and is most dominant in the intercolpial areas; the latter can be seen in the fossil pollen. The flanks of the equatorial apices in the equatorial plain are straight in *Helixanthera* and the fossil, whereas they are continuously curved in *Amyema*. In addition, the polar depression in *Helixanthera* and the fossil are identical in all details in SEM (Figs. 6C, 6D, 6F), whereas in *Amyema* the polar margo is more distinct and shows three small triangular protrusions (Fig. 6E).

Use as age constraint

The phylogenetic position of *Helixanthera* within the core Lorantheae is uncertain. Nucleotide data has been produced for three species including *Helixanthera kirkii*, but the data are partly problematic and too fragmentary. *Helixanthera kirkii* (only nuclear data available, only species palynologically studied so far) nests deep within the Lorantheae core clade, and *H. parasitica* Lour. (only plastid data available) is sequentially divergent from all Lorantheae and effectively unplaced (see Fig. 7 and File S1 for further details). The third and best covered species, *H. coccinea* Danser, groups with species of *Dendrophthoe* in agreement with the current systematic scheme, but its pollen is yet to be studied. Thus, *Helixanthera* has not been included in the taxon-reduced species-consensus dataset used here for the molecular dating. A conservative use could be constraining the minimum age of the MRCA of the Clade J (i.e. Scurrulinae, Dendrophthoinae, Emelianthinae, and Tapinanthinae; see Discussion).

INFERENCES

Basic signal in the harvested molecular data

Our inferences, based on species-consensus sequences and different sets of data (see File S1 and files included in OSA), did not reveal any well-supported conflict between the nuclear and plastid gene regions (Fig. 7). Inclusion or exclusion of the most divergent, length-polymorphic non-coding (plastid) trnL/LF region showed little effect on the optimised ML topologies and BS support values. When not including any long-branching outgroups, the data largely fails to group the root parasitic taxa. Hence, there is a lack of

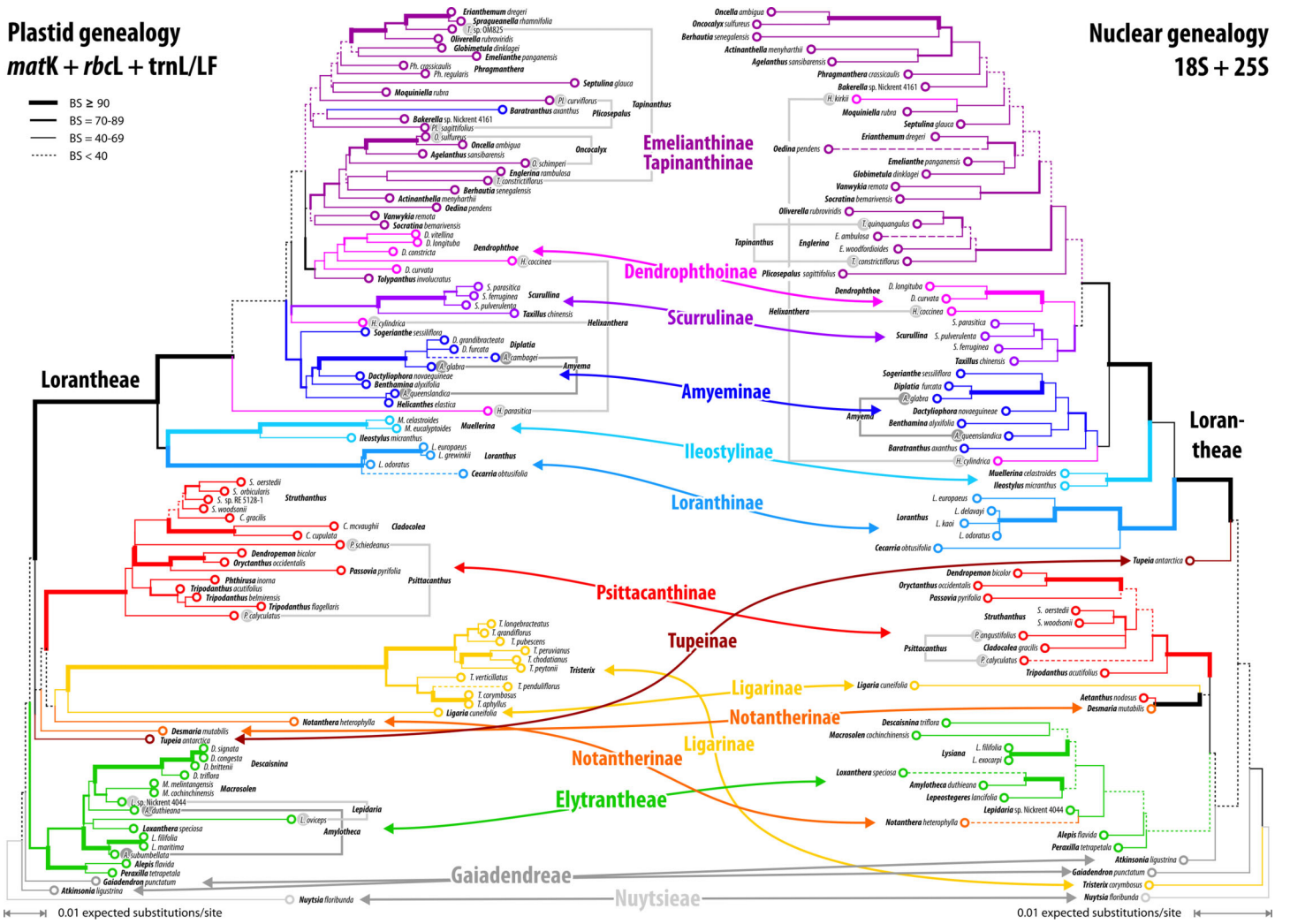

Figure 7 **Plastid and nuclear species trees for the complete taxon set.** No high-supported conflict is found; both datasets recognise the same main clades, while failing to resolve most of the deeper inter-clade relationships. Particularly, the phylogenetic position of tribes/subtribes with few, often monotypic, genera (root parasitic Nuytsieae, Gaiadendreae, aerial parasitic Ligarinae, Notantherinae, and Tupeinae) is essentially unresolved. Local differences in the topologies and odd placements are often related to species with large amount of missing data. Stippled terminal branches have been reduced by factor 2.

support for a root parasitic grade. An according subtree (e.g. *Su et al., 2015*: Fig. 1B) draws its support exclusively from the *matK* gene data and is enforced if long-branching sistergroups of the Loranthaceae are included (*Grímsson, Grimm & Zetter, 2017*: File S6). Overall, the single- and oligo-gene species-consensus trees showed the same principal topology as earlier found using genus-consensus sequences (*Grímsson, Grimm & Zetter, 2017*: Figs. 2, 3). However, species of the same genus were not necessarily reconstructed as siblings. In the case of *Helixanthera, Psittacanthus* (nuclear and plastid data), and *Plicosepalus* (plastid data only), the branches separating the putative siblings received no high support, while the opposite was true for *Amyema, Tapinanthus* (nuclear and plastid data), *Amylotheca, Lepidaria,* and *Oncocalyx* (plastid data only). In terms of genetic-phylogenetic distances, the species of *Helixanthera* show the least coherence at the

genus level. Aside from this, several clades were consistently reconstructed and usually received moderately high to unambiguous support (BS $\geq$ 70) from different data sets (Fig. 7): (1–4) the Old World Lorantheae with three subclades (Loranthinae, Ileostylinae, core Lorantheae), (5, 6) the Amyeminae (except *Baratranthus axanthus*) and Scurrulinae within the core Lorantheae; (7) the New World Psittacanthinae (except for *Aetanthus*, which is poorly sampled in our data set); and (8) the Elytrantheae (poorly supported based on nuclear data due to faint discriminating signals). The positions of the other mostly monotypic genera of the family remained unresolved; alternative splits representing deep relationships generally received low support. Bayesian inference is more decisive, with PP ~ 1.00 found for all major splits with moderately high to high BS support ($BS_{ML} \geq 77$) and several splits with low BS support (see Materials and Methods). Some of the deepest splits that received $BS_{ML} < 35$, received PP > 0.5 (all alternatives with PP < 0.2). A split between root and aerial parasites is not supported by any analysis with BS_{ML}/PP > 20/0.2. A detailed account regarding topological ambiguity of inferences using the currently available molecular data can be found in File S5.

The divergence in the covered gene regions is substantial (see branch-lengths in Fig. 7); the resulting terminal 'noise' appears to obscure any signal that may allow for the discrimination of deeper phylogenetic splits. This may explain to some degree, in addition to the relatively high proportion of missing data, the low resolution capacity of comprehensive species-level data sets. When the taxon set was reduced to only those species with full data coverage, support along the backbone and towards the leaves of the Loranthaceae tree increased. This reduction also showed a positive effect on the dating: using the complete taxon set and matrices with numerous data gaps, ESS values converged very slowly (rooting scenarios 1 and 3) or not at all (rooting scenario 2; see also File S1).

Alternative clock-based roots

For four of the five comprehensive datasets (all taxa, different sets of gene samples), the clock-inferred root was placed between the predominately Old World Lorantheae and a mostly southern hemispheric, American-Australasian clade collecting all three root parasitic genera and the members of the other two aerial parasitic tribes, the (probably paraphyletic) Psittacantheae and (putatively monophyletic) Elytrantheae (Table 2). In the case of the most-inclusive data set (all taxa, all gene regions), the root was shifted by two nodes and placed within the Lorantheae subtree, splitting the genetically divergent subtribes Loranthinae and Ileostylinae from the remainder of the Lorantheae (= Clade J according to *Vidal-Russell & Nickrent, 2008a*). The subsequent evolutionary scenario would imply that root parasites and other southern hemispheric lineages share an ancestor with only the Loranthinae and Ileostylinae. This would mean a paraphyletic Lorantheae tribe, which is highly unlikely (*Nickrent et al., 2010*; *Su et al., 2015*; *Grímsson, Grimm & Zetter, 2017*). Thus, this alternative root was not further considered. In contrast to these roots, the taxon-reduced, less 'gappy' dataset (42 species covering, at least partly, all included gene regions) recovered the outgroup-inferred root, with *Nuytsia* as sister to all other loranths.

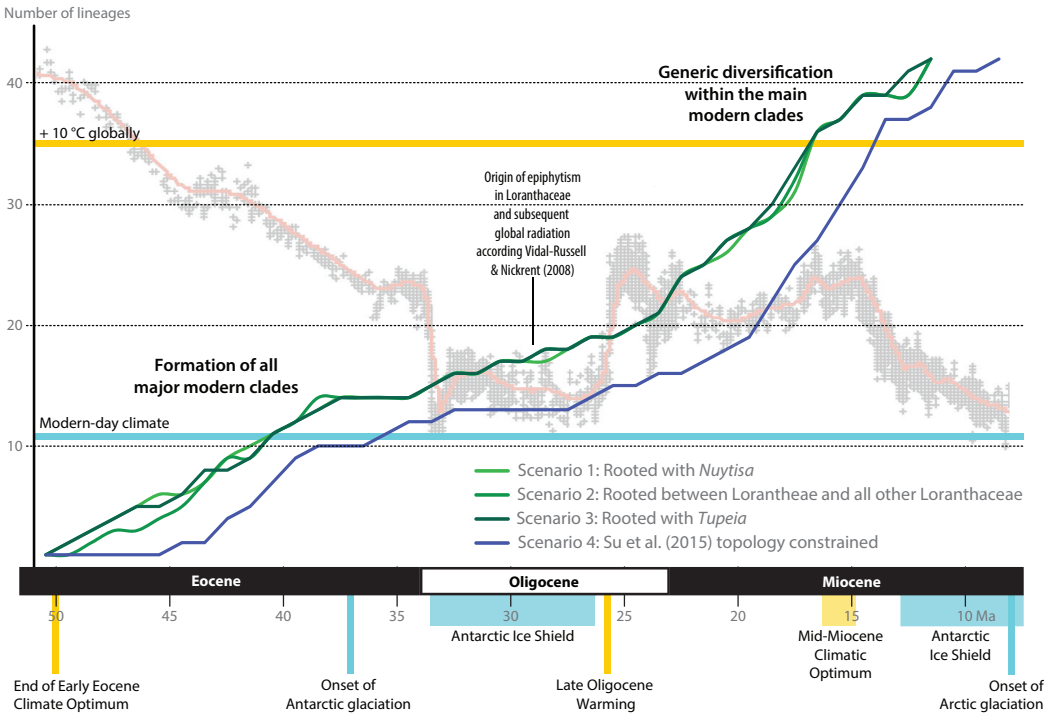

Figure 8 Lineage-through-time plots for Loranthaceae as inferred based on three different rooting scenarios or enforcing the topology of *Su et al. (2015)*; scenario 4*)*. Background shows the stable-isotope-based (marine sediments) global temperature curve with main climatic events annotated at the bottom (after *Zachos et al., 2001*). Increased diversification of Loranthaceae is inferred for time-scales when the global mean temperature was at least ~5° C higher than today (middle to late Eocene; late Oligocene to mid-Miocene).

Temporal framework for pollen evolution in Loranthaceae

Following our clock-rooting results and those of earlier studies, we applied three different root constraints to judge potential effects of topological uncertainties regarding the primary relationships on the dating estimates (Figs. 8–9; Table 3). In addition, we constrained our data to the topology of the Loranthaceae subtree as shown in *Su et al. (2015*; scenario 4*)*, which—according to an expert on the group—is the most correct one to date (but see *Grímsson, Grimm & Zetter, 2017*: File S6). We find that independent of the position of the root and exact structure of the backbone topology, primary divergences in Loranthaceae were terminated by the end of the Eocene at the latest (Table 3). The posterior estimates of the evolutionary rates per gene were equivalent in all rooting scenarios (Table 4) and slightly higher for the fourth scenario in which the topology was constrained to the one of *Su et al. (2015)*. The estimated rates for *mat*K and trnL/LF were within the range of mean rates reported for coding and non-coding plastid gene regions (7×10^{-5}–8×10^{-3} substitutions per million years; e.g. *Wolfe, Li & Sharp, 1987*; *Palmer, 1991*; *Chen et al., 2012*; see also *Guzmán & Vargas, 2010*; *Désamoré et al., 2011*; *Lockwood et al., 2013*). The robustness of our estimations are further supported by the fact that the observed phases of increased diversification (number of

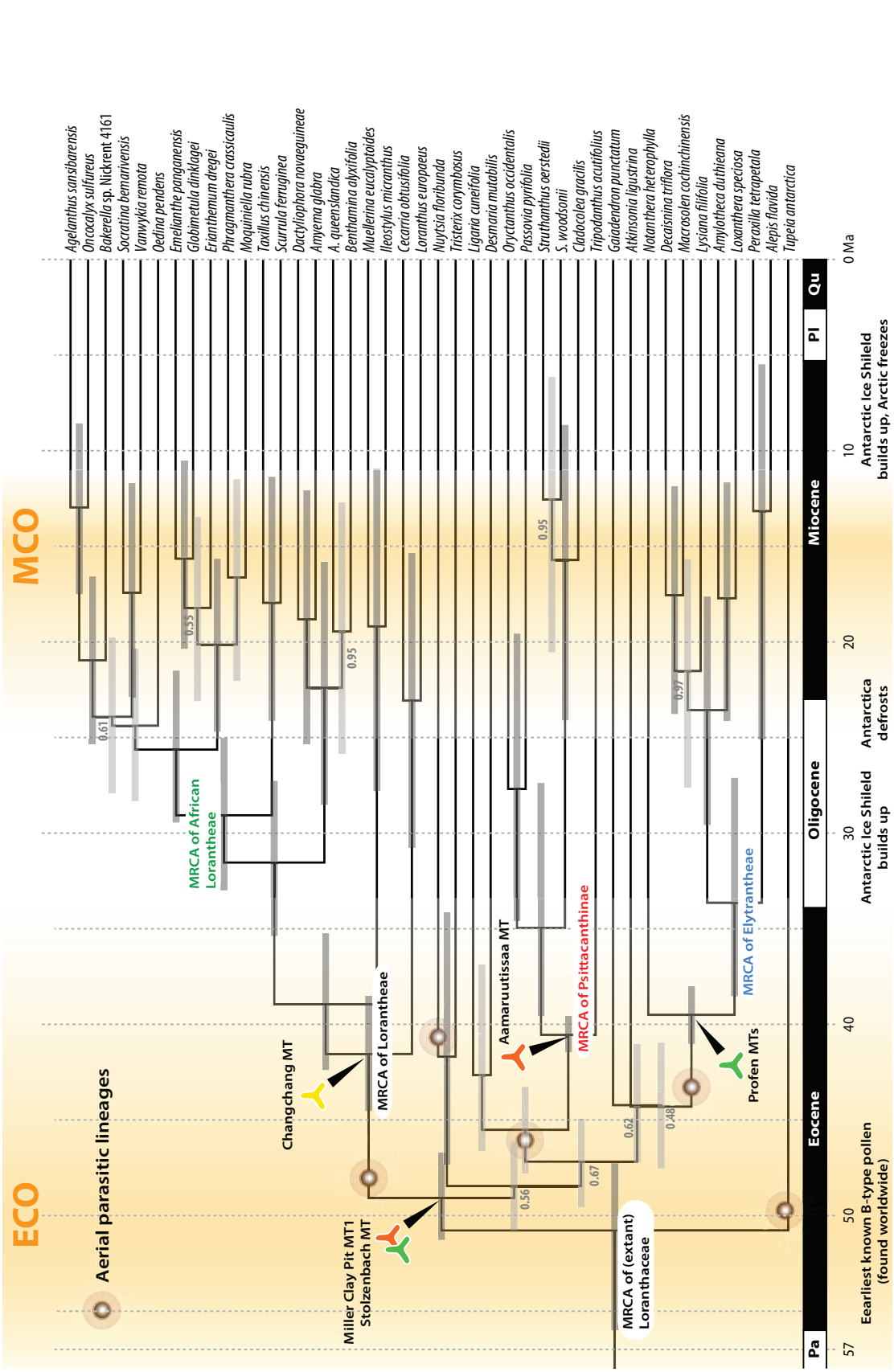

Figure 9 A dated phylogeny of Loranthaceae using the pollen-informed root (rooting scenario 3). The chronogram is based on a concatenated data set including two nuclear ribosomal RNA genes (18S and 25S rDNA), two coding plastid genes (*rbcL*, *matK*) and the trnL/LF region. The taxon set has been reduced to species with sufficient data, i.e. data covering all included gene regions. Node heights (divergence ages) are medians, grey bars indicate the 95%-highest-posterior-density intervals; labels at branches indicate posterior probabilities for those branches that did not receive unambiguous support. Triangular doodles represent pollen used as age priors for the according nodes: green—Central Europe; red—North America (including Greenland); yellow—East Asia. ECO, Eocene warm phase; MCO, Miocene warm phase (see Fig. 8).

Table 3 Results of the dating analyses using the reduced taxon data set and different rooting scenarios.

Node	Rooting scenario 1			Rooting scenario 2			Rooting scenario 3			Scenario 4			Av. Medians	Abs. min	Corresponds to	
	L.b.	Median	U.b.	L.b.	Median	U.b.	L.b.	Median	U.b.	L.b.	Median	U.b.				
Loranthaceae crown	52.6	50.1	47.8	51.5	**49.1**	46.9	56.1	50.8	47.3	48.0	45.4	43.0	**48.9**	43.0	Earliest	Lutetian
Nuytsia root	52.6	50.1	47.8	50.4	48.1	45.9	47.4	41.6	34.2	48.0	**45.4**	43.0	**46.3**	34.2	Latest	Priabonian
Atkinsonia root	46.8	**43.8**	40.7	45.7	43.1	40.5	47.5	44.3	40.9	45.9	43.9	42.0	**43.8**	40.5	Early	Bartonian
Gaiadendron root	46.5	**43.7**	40.7	45.7	43.1	40.6	47.4	44.3	41.1	45.1	43.2	41.5	**43.6**	40.6	Early	Bartonian
Tristerix root	52.2	49.7	47.3	48.0	**44.4**	38.9	47.4	41.6	34.2	40.4	37.0	31.9	**43.2**	31.9	Latest	Priabonian
Tupeia root	49.7	47.2	44.8	48.0	**44.4**	38.9	56.1	50.8	47.3	42.2	39.1	32.7	**45.4**	32.7	Late	Bartonian
MRCA (aerial parasitic) new world taxa	52.2	49.7	47.3	48.7	**46.8**	44.9	50.8	48.5	46.2	42.8	41.4	40.2	**46.6**	40.2	Mid	Lutetian
MRCA *Desmaria–Ligaria*	46.0	**42.2**	36.3	45.2	41.5	36.0	46.7	42.6	36.9	42.8	41.4	40.2	**41.9**	36.0	Mid	Priabonian
Notanthera + Elytrantheae root*	46.8	**43.8**	40.7	45.7	43.1	40.5	47.5	44.3	40.9	[N/A]			**43.7**	40.5	Early	Bartonian
MRCA *Notanthera* + Elytrantheae*	41.0	**39.5**	38.0	40.9	39.4	37.8	41.0	**39.5**	38.0	44.1	42.5	41.1	**40.2**	37.8	Latest	Bartonian
Notanthera + Psittacanthinae root*	[N/A]			[N/A]			[N/A]			42.2	**40.9**	39.7	**40.9**	39.7	Early	Bartonian
MRCA *Notanthera* + Psittacanthinae*	48.6	46.4	44.3	47.4	**45.5**	43.8	49.6	47.2	44.9	41.5	40.5	39.5	**44.9**	39.5	Early	Bartonian
Psittacanthinae root	47.1	45.0	43.0	46.2	**44.4**	42.6	47.9	45.5	43.4	41.5	40.5	39.5	**43.8**	39.5	Latest	Lutetian
Psittacanthinae crown	41.4	40.4	39.5	41.3	**40.3**	39.4	41.5	40.6	39.6	29.8	22.8	16.7	**36.0**	16.7	Mid	Bartonian
Elytrantheae root	41.0	**39.5**	38.0	40.9	39.4	37.8	41.0	**39.5**	38.0	42.6	41.2	39.6	**39.9**	37.8	Latest	Bartonian
Elytrantheae crown	38.5	33.4	26.7	38.2	**33.1**	26.6	38.5	33.5	27.0	35.1	27.2	20.2	**31.8**	20.2	Early	Chattian
Lorantheae root	49.7	**47.2**	44.8	51.5	49.1	46.9	51.4	49.1	46.8	42.6	41.2	39.6	**46.7**	39.6	Mid	Lutetian
Lorantheae crown	44.2	**41.1**	37.8	45.1	41.8	38.5	44.7	41.6	38.6	38.1	35.9	33.5	**40.1**	33.5	Earliest	Priabonian
Core Lorantheae crown	35.2	**31.2**	27.0	35.9	31.6	27.4	35.6	31.7	27.4	29.8	26.5	22.9	**30.2**	22.9	Early	Chattian

Notes:

Cells with same background colour refer to the same node. Medians closest to the arithmethic mean of all four scenarios (column 'Av. Medians') in bold, minimal age scenarios for each node (column 'Abs. min') highlighted by blue colour.

U.b., upper boundary; L.b., lower boundary, of the 95%-highest-posterior-density interval; MRCA, most recent common ancestor (can be inclusive or exclusive).

* If topology is unconstrained, *Notanthera* is placed as sister to Elytrantheae (BS_{ML} = 57; PP = 1.00); in Scenario 4, *Notanthera* is constrained as sister of Psittacanthinae (topological constraints derived from the tree shown in *Su et al., 2015*.

coexisting lineages) and stagnation concur with key events in Cenozoic climate and vegetation evolution (Fig. 8). Most crown group radiation, the formation of the modern genera, apparently happened no later than the Miocene. Based on the limited species coverage, it is impossible to estimate when intra-generic radiation stepped in, and at which point closer related genera became isolated and diverged.

Comparison of Bayes factors showed that rooting scenario 3, the pollen-informed root, is decisively superior (according *Kass & Raftery, 1995*) than the tested alternatives (Table 5). Thus, we chose rooting scenario 3 as the basis for our discussion and conclusion. The divergence between *Tupeia* (A-type pollen) and Loranthaceae with B-type pollen is placed in the early Eocene (~50 Ma; Fig. 9, Table 3). A primary radiation followed shortly after (less than 2 myrs), and involved the formation of an essentially Old World

Table 4 Estimated substitution rates (per million years) for each of the used genetic markers.

Genetic marker	Rooting scenario 1	Rooting scenario 2	Rooting scenario 3	Scenario 4
	Median ucld.mean			
18S rDNA	2.5×10^{-4}	2.5×10^{-4}	2.5×10^{-4}	2.9×10^{-4}
25S rDNA	6.5×10^{-4}	6.6×10^{-4}	6.3×10^{-4}	8.2×10^{-4}
*mat*K	10.1×10^{-4}	10.1×10^{-4}	10.0×10^{-4}	11.7×10^{-4}
trnL/LF[a]	12.9×10^{-4}	13.1×10^{-4}	12.8×10^{-4}	15.5×10^{-4}

Note:
Estimates are provided for all four tested topological hypotheses (rooting scenarios 1–3, and scenario 4 constraining the topology of *Su et al. (2015)*).
[a] Includes the *trn*L intron and downstream-located (5') *trn*L exon (can be incomplete) and *trn*L–*trn*F spacer (complete).

Table 5 Ranking of the four tested topological configurations (three rooting scenarios, and scenario 4 constraining the topology of *Su et al., 2015*).

Rank	Scenario	Stepping-stone		Path-sampling	
		MLE	BF	MLE	BF
1	Rooting sc. 3 *Tupeia* sister to rest	−29457.1		−29456.0	
2	Rooting sc. 1 *Nuytsia* sister to rest	−29461.0	7.87	−29460.0	8.08
3	Scenario 4 *Su et al. (2015)*	−29464.3	14.53	−29463.3	14.61
4	Rooting sc. 2 (Lorantheae sister to rest)	−29466.3	18.54	−29465.7	19.43

Note:
Ranking is based on marginal likelihood estimates (MLE) and Bayes factors (BF), calculated using two approaches, stepping-stone and path-sampling, implemented in BEAST (*Baele et al., 2012*, *2013*).

(Lorantheae) and New World clade (root parasites, Elytrantheae, Psittacantheae). Subsequently, the first divergences in the New World clade occurred (≥43 Ma; Fig. 9). Crown group radiation in the Lorantheae started in the late Eocene (≥38 Ma) at the latest; the subclades and monotypic lineages (subtribes Psittacanthinae, Ligarinae, Notantherinae) of the probably paraphyletic Psittacantheae diverged at about the same time. A second major radiation phase took place ~10 myrs later (latest in the Oligocene) and involved the Old World core Lorantheae (subtribes Amyeminae, Dendrophthoinae, Emelianthinae, Scurrulinae, Tapinanthinae) and New World Elytrantheae. Crown group radiation, the formation of lineages equalling most modern genera, commenced at about the same time and lasted till the mid-Miocene (≥9 Ma). In general, the genera root deeper, i.e. are older, in the (mostly) South American Psittacanthinae than in the Old World Lorantheae sublineages and the (mainly) Australasian Elytrantheae. Generic diversification culminates in the early to mid-Miocene, a time of ameliorated global climate (*Zachos et al., 2001*; see last section of Discussion).

Historical Biogeography

Pollen studied using SEM and subsequent node dating (Figs. 8, 9; Table 3) indicate that several major lineages of Loranthaceae were present in the Northern Hemisphere by the

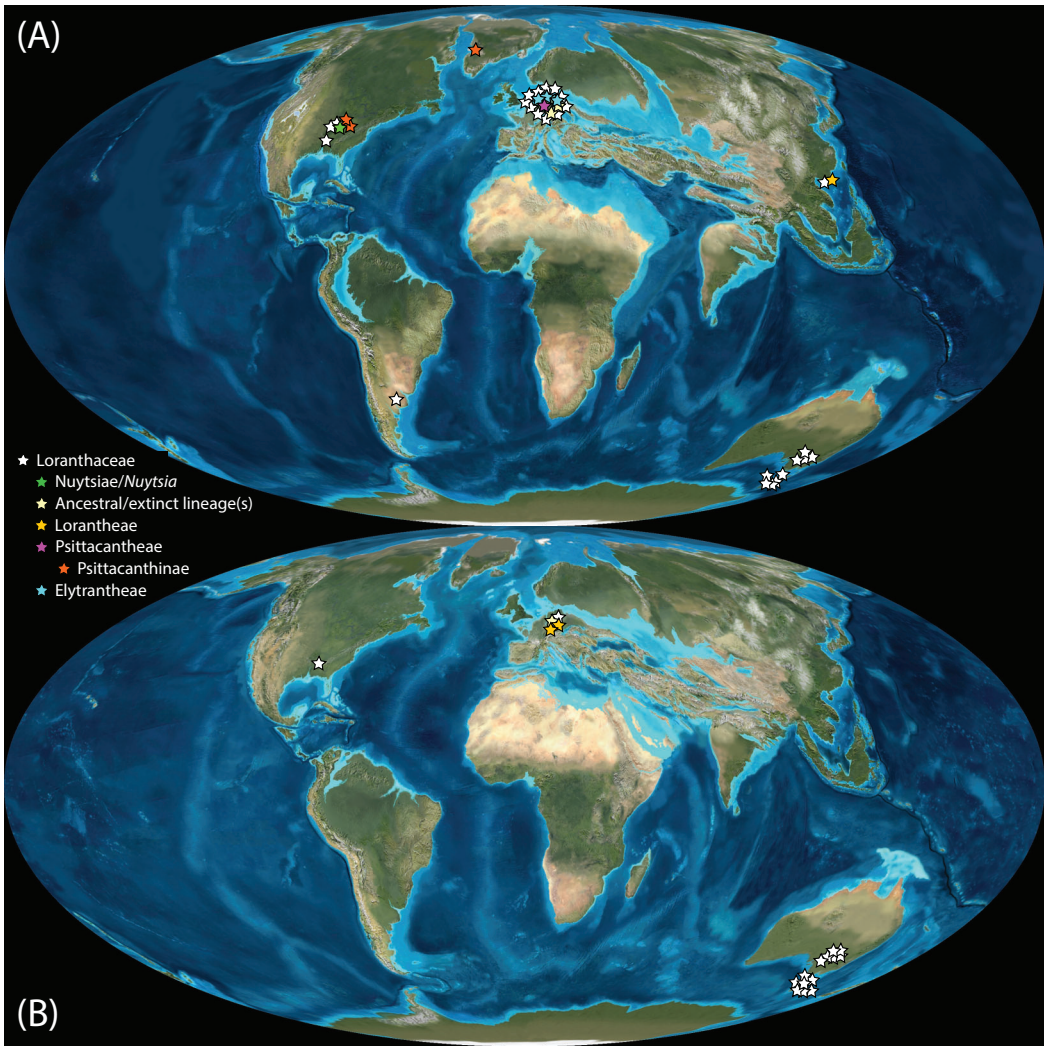

Figure 10 Global distribution of Loranthaceae in the Paleogene, evidenced based on unequivocal palynological records. (A) Eocene. (B) Oligocene. Maps are Mollweide views, projected through the prime meridian (*Blakey, 2008*; Global DVD © 2011 Colorado Plateau Geosystems Inc.).

middle Eocene (Fig. 10A). The Eocene pollen record includes representatives of extinct or ancestral lineages with affinities to root-parasitic genera such as *Nuytsia*/Nuytsieae, but possibly also to the Lorantheae (Miller Clay Pit MT1, Stolzenbach MT, Profen MT1). In addition, today's exclusively epiphytic lineages are present: Psittacanthinae in North America/Greenland (Miller Clay Pit MT2, MT3, Aamaruutissaa MT), *Notanthera* and Elytrantheae in Central Europe (Profen MT3, MT4 and MT5), and core group Lorantheae in East Asia (Changchang MT). All these records represent the earliest unequivocal fossil records of their respective groups. At least one of these lineages, the ancestral/extinct lineage bridging the root parasites and Lorantheae, persisted in Eurasia during the late Eocene and Oligocene (Theiss MT, Altmittweida MT; Fig. 10B) until today. These younger pollen types, which were not used as node age priors, are in good agreement with the dating estimates (Fig. 9). Furthermore, we noticed that none of the

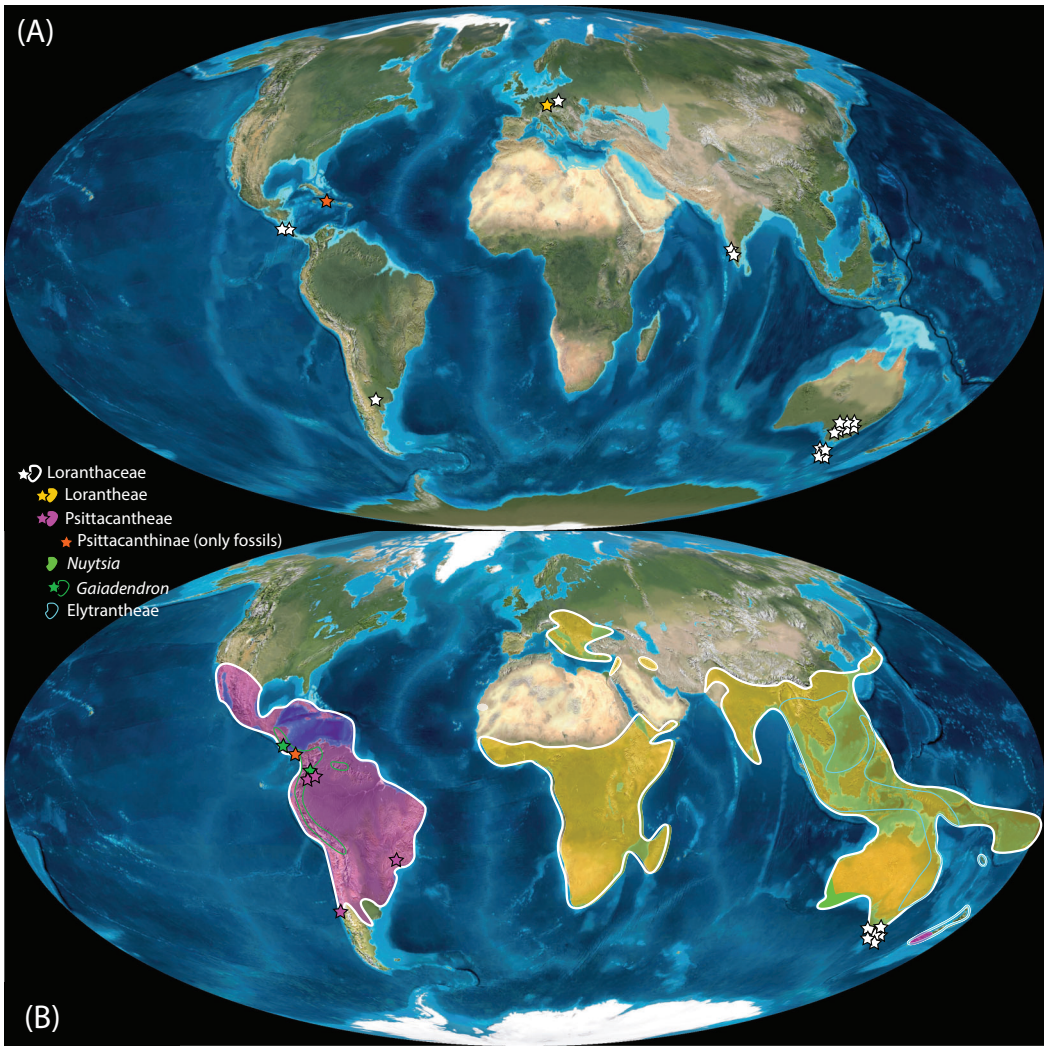

Figure 11 Global distribution of Loranthaceae in the Neogene, evidenced based on unequivocal palynological records. (A) Miocene. (B) Pliocene to recent. Asterisks indicate fossil occurrences; shaded/circum-lined areas in (B) reflect the modern-day distribution. Maps are Mollweide views, projected through the prime meridian (*Blakey, 2008*; Global DVD © 2011 Colorado Plateau Geosystems Inc.).

putatively derived pollen morphologies characteristic of certain members of the Psittacanthinae (compact B-type, C-type and D-type pollen) and Lorantheae (Loranthinae, Tapinanthinae-Emelianthinae; ± compact B-type pollen, B-type pollen with minute sculpturing, heteropolar grains) have been found (so far) in the older strata. Pollen records from the Miocene onwards, studied using LM and possibly representing a large range of Loranthaceae lineages with a B-type pollen, fall within the modern distribution area (Fig. 11), and potentially include such B types (File S4). The most derived C- and D-type pollen characteristic for *Dendropemon, Passovia* p.p. and *Oryctanthus*, which should be straightforwardly recognised with LM only, is rare and only known from late Miocene/sub-recent sedimentary rock formations. The dated trees predict an Oligocene/early Miocene age for the MRCA of *Passovia pyrifolia* and

Oryctanthus (Fig. 9). If Loranthaceae with A-type pollen contributed to the pollen record of the family, they would not have been recognised as Loranthaceae, hence, are not included in our maps and File S4 (Figs. 10, 11).

Well-resolved major clades of Loranthaceae are restricted to one or two adjacent biogeographic regions (Fig. 11). Except for *Nuytsia*/Nuytsieae (today only found in southwestern Australia), the fossil pollen records essentially reflect the modern situation, only extending the range of the respective New World and Old World lineages to higher latitudes of the Northern Hemisphere.

DISCUSSION

Diagnostic value of Loranthaceae pollen for tracing modern lineages back in time

Pollen of various modern Loranthaceae have been studied using light (LM), transmission electron microscopy (TEM) and scanning-electron microscopy (SEM) (*Feuer & Kuijt, 1978*, *1979*, *1980*, *1985*; *Kuijt, 1988*; *Liu & Qiu, 1993*; *Han, Zhang & Hao, 2004*; *Roldán & Kuijt, 2005*; *Caires, 2012*; *Grímsson, Grimm & Zetter, 2017*). In general, pollen of Loranthaceae—and other Santalales—reflect phylogenetic relationships and genetic-phylogenetic distances (*Grímsson, Grimm & Zetter, 2017*), which make them a valuable asset for biogeographic and dating studies. Some genera of putatively early diverging Loranthaceae lineages such as *Nuytsia* (monotypic Nuytsieae), *Atkinsonia* (bitypic Gaiadendreae, not resolved as clade in the molecular trees), the Psittacantheae *Notanthera* (bitypic Notantherinae), *Ligaria* and *Tristerix* (Ligarinae, not resolved as sibling genera), and *Tripodanthus*, *Dendropemon*, *Orycanthus* and *Passovia* p.p. (Psittacanthinae), show unique pollen types that have not been found in any other studied genus so far. Moreover, there is no indication that identical/highly similar pollen types evolved convergently in non-related Loranthaceae (or other Santalales). Non-unique pollen types are typically found in genera which are either part of the same, well-supported molecular clade (core Lorantheae; Elythrantheae; Psittacanthinae subclades), or shared with genera where the molecular data is indecisive regarding their exact phylogenetic position (*Grímsson, Grimm & Zetter, 2017*; this study).

Even though the modern situation makes it unlikely that—in the past—extinct lineages of Santalales or Loranthaceae have produced pollen mimicking those of modern, extant, but not closely related lineages, one needs to consider the possibility that a modern genus may have kept a more primitive ('plesiomorphic') pollen type of its evolutionary lineage. The Eocene and Oligocene pollen grains documented in this study show morphologies (1) not found in any modern taxon studied so far (Stolzenbach MT, Profen MT1, Theiss MT), or (2) found exclusively in a single modern genus (monotypic *Nuytsia*: Miller Clay Pit MT1, *Tripodanthus* with three extant species: Miller Clay Pit MT2, MT3, Aamaruutissaa MT; monotypic *Notanthera*: Profen MT2; phylogenetically problematic, see Fig. 7; *Helixanthera*: Altmittweida MT), or (3) are limited to a modern lineage (Elytrantheae: Profen MT3–5; core Lorantheae: Changchang MT) with none of the other modern species studied so far having an identical pollen. On the other hand, we found no

pollen in our Eocene and Oligocene assemblages representing current-day diverse and widespread genera (such as *Loranthus* in Eurasia).

Extinct or ancestral pollen morphs of the Eocene and Oligocene of Europe

The shared pollen type of the South American root parasite *Gaiadendron* and the eastern Australian Lorantheae *Muellerina* (one of two genera in the subtribe Ileostylinae; the other has not been palynologically studied thus far) is a candidate for an ancestral, primitive and shared ('symplesiomorphic') morphology. The pollen of these two genetically and morphologically distinct modern genera are indistinct (*Nickrent et al., 2010*; *Su et al., 2015*: Fig. 2; *Grímsson, Grimm & Zetter, 2017*). The distinctly striate margo is a feature only seen in a few isolated, early diverging (Eocene) modern species/genera of ambiguous phylogenetic affinity (Fig. 9; Table 3). So far, no modern species showed an intermediate pollen type between the putatively plesiomorphic *Gaiadendron–Muellerina* pollen and the derived pollen characterising other members of the Lorantheae, e.g. the characteristically weakly oblate pollen of *Loranthus*. The Stolzenbach MT, Profen MT1, and Theiss MT of the Eocene and Oligocene of central Europe are equally small and share certain ornamental characteristics with the pollen of *Gaiadendron–Muellerina* such as a distinctly striate margo. Deviating features, e.g. more minute sculpturing of the mesocolpium, are shared with other members of the Lorantheae. This could make them candidates for an extinct lineage related to Lorantheae or ancestors of the Lorantheae subclades. At about the same time, more derived Lorantheae pollen grains can be found in the Eocene of East Asia (Changchang MT) and the Oligocene of Germany (Altmittweida MT), with clear affinities to the core Lorantheae. This provides conservative minimum estimates for the Lorantheae crown age, i.e. the divergence between Loranthinae, Ileostylinae, and core Lorantheae. Our dating estimates also indicate that there was a time gap of ca. 10 myrs between the formation and initial radiation of the Lorantheae and their subsequent diversification (Fig. 9; Table 3). Our current working hypothesis is that the Stolzenbach MT, Profen MT1, and Theiss MT, do in fact represent extinct sister lineages or precursors of the modern Old World Lorantheae (e.g. the Loranthinae). Whether these Loranthaceae extended into Africa or not, is unknown. The divergence between the East Asian Scurrulinae and the mostly African Tapinanthinae and Emelianthinae is placed in the Oligocene (Fig. 9), a time when substantial global cooling triggered the retreat of subtropical and tropical forests to low latitudes (*Mai, 1995*; *Zachos et al., 2001*). This event may have triggered the isolation between both clades and lead to the extinction of the ancestral pollen morphologies. Unfortunately, Africa is palaeo-palynologically understudied, so we do not know at which time the African Lorantheae with pollen grains typical for their modern members established. SEM studies of African palynofloras with Loranthaceae pollen from the Oligocene to Pliocene are desperately needed.

Pollen of Tripodanthus*, a putative living palyno-fossil*

Another case of a modern genus that conserved a primitive pollen morphology is evident from the Eocene pollen from North America and Greenland (Miller Clay Pit MT1, MT2; Aamaruutissaa MT). These pollen are highly similar to identical to pollen of two

out of three species of the modern South American genus *Tripodanthus*; the third species has a more compact pollen somewhat similar to that of small-flowered species of the Psittacanthinae (Fig. S4; *Feuer & Kuijt, 1985*; *Roldán & Kuijt, 2005*; *Amico et al., 2012*; *Grímsson, Grimm & Zetter, 2017*). *Tripodanthus* is one of the earliest diverging Psittacanthinae (Figs. 7, 9; *Vidal-Russell & Nickrent, 2008a*; *Grímsson, Grimm & Zetter, 2017*). Pollen in the other represented genera of the Psittacanthinae (*Passovia, Dendropemon, Struthanthus, Oryctanthus*) appear strongly derived in comparison to that of *Tripodanthus* and part of *Psittacanthus* (*Feuer & Kuijt, 1979*, *1985*), and include types that could be identified under LM. However, such pollen have not yet been reported from the fossil record except for the youngest strata (*Bartlett & Barghoorn, 1973*; *Graham, 1990*: File S4). Moreover, the current molecular data covers only a very limited fraction of the species in the Psittacanthinae, a clade palynologically well studied and diverse. So, at the moment, we lack a sound molecular framework to test hypotheses about pollen evolution within the group, and the group is genetically undersampled. Even so, our set of ML inferences highlights the shortcoming of the current generic concepts used for the group. So far, *Tripodanthus* is the only Psittacanthinae genus where the species/sequenced individuals show a relatively high topological coherence; an according, exclusive clade is supported by varying support (Fig. 7; Files S1, S5).

The Eocene *Tripodanthus*-like pollen of North America and Greenland might have been produced by extinct or ancestral members of the Psittacanthinae, rather than an ancient member of the *Tripodanthus*-lineage. It may merely confirm the existence of the New World Psittacanthinae clade in the Eocene of North America and Greenland, and should be linked with a deeper node. Using LM, Loranthaceae pollen (*Gothanipollis* sp.) has been recorded from North and South America from the early Eocene onwards (File S4 lists 17 records), which may well reveal different forms of Psittacanthinae pollen, or of less diverse New World lineages when re-studied using SEM.

Data-inherent shortcomings

The data assembled for our study from gene banks do not allow for conclusions at and below the genus level to be drawn. Genus-level data are limited, and in several cases where more than a single species (or individual) has been sequenced from the same genus, the genera do not show a high coherence when it comes to tree inferences (Fig. 7). This will become a problem when studying pollen grains from younger strata, which, increasingly, may show forms identical to one or more modern genera. For instance, our assessment of the Altmittweida MT is based on its similarity to the pollen of *Amyema* and *Helixanthera* figured in *Grímsson, Grimm & Zetter (2017)*. In that study, material was used from vouchers identified as *A. gibberula*, the only species of the Amyeminae clade studied so far palynologically, and *Helixanthera kirkii.* According to our species-level analyses, species of neither of the two genera are resolved as sibling species. As exemplified in Fig. 7, the two or three sequenced species of *Amyema* are resolved at different placements in the Amyeminae subtree, but *A. gibberula* has not been sequenced at all. *Helixanthera kirkii* has only been sampled for nuclear data, and is placed far (phylogenetically speaking) from its congeners, which are scattered across the core Lorantheae subtree. Lacking any

comparative data, it cannot be judged if these placements are genuine, or if one (or several) of the species (sequenced individuals) were misidentified/-associated (generic concepts are volatile in Loranthaceae, see synonymy lists provided by *Tropicos.org, 2016*). Thus, based on the available pollen of the Lorantheae and their established genetic affinities as members of the same clade, we can only assume with some certainty that the Altmittweida MT is a likely representative of the core Lorantheae, but not if it is a congener of *Helixanthera*, or more closely related to part of that genus. We also cannot judge to which degree *Helixanthera* pollen can be considered derived/unique enough within the core Lorantheae to warrant the association of a fossil pollen with a single extant genus.

Furthermore, we can only rely on fossil pollen of several northern hemispheric localities; localities we have been studying in the recent years. But most of the extant, and potentially extinct, diversity of Loranthaceae lies in the Southern Hemisphere (Figs. 10–11). South America, and in particular Africa, are much less studied palynologically than e.g. Europe, and the tradition of using SEM to study fossil pollen records is scant or absent in the Americas and Australasia (but see *Ferguson et al., 2009*; *Bouchal, Zetter & Denk, 2016*; *del Carmen Zamaloa & Fernández, 2016*). Nevertheless, there are records of Loranthaceae pollen from these areas, and if Antarctica is included (File S4), these records cover anything between the early Eocene and Holocene. Moreover, pollen assigned to Santalaceae or Viscaceae under LM may in fact be Loranthaceae Pollen Type A. Re-studying at least some of these assemblages using high-resolution SEM photography could provide much needed evidence for the distribution of different Loranthaceae lineages back in time. A more detailed and comprehensively studied pollen record at a global scale would also provide the necessary number of fossils to put forward and test explicit phylogeographic scenarios for the family. In the case of South America, particular fossil pollen can be straightforwardly compared to the substantial variation seen in the modern genera and species (seminal works of *Feuer & Kuijt, 1979*, *1980*, *1985*). It would be most interesting to pinpoint the earliest occurrences of the compact B-type pollen characteristic of the *Cladocolea-Struthanthus* lineage or the strongly derived C- and D-type pollen of the *Passovia pyrifolia-Dendropemon-Orycthanthus* clade. However, we are missing comprehensive molecular data on the Psittacanthinae at the intra-generic level and on species included in *Passovia* and *Phthirusa* (according *Kuijt, 2011*; see e.g. Fig. 7). A detailed molecular-phylogenetic framework would be necessary to depict evolutionary trends in pollen morphology of this group and to identify ancestral, more primitive (plesiomorphic) vs. modern, derived (apomorphic) pollen morphs of this lineage in the fossil record. Correlation of such data with palaeovegetational evidence (accompanying flora, in particular availability of mid- to high-canopy trees), may help to assess if the shift from root to aerial parasitism in currently exclusively aerial parasitic Loranthaceae lineages occurred before or after their establishment.

Due to the data-related limitations regarding both the molecular data and the fossil record, our dating analysis set-up can only provide absolute minimum estimates for divergence ages in the Loranthaceae. In a recent study on Osmundaceae, we observed that

uncorrelated clock-inferred dates deviated from dates inferred with the recently proposed fossilised-birth-death dating approach (FBD; *Heath, Huelsenbeck & Stadler, 2014*), with the former tending to underestimate age (*Grimm et al., 2015*). In contrast to traditional node dating, FBD dating recruits the entire fossil record of a focal group and seems to outperform node dating in simulation and with real-world data (*Heath, Huelsenbeck & Stadler, 2014*; *Grimm et al., 2015*; *Renner et al., 2016*). In the case of Loranthaceae, the coverage of lineages with fossils and of the modern taxonomic diversity is insufficient for the application of FBD, although this approach would allow for a more appropriate handling of the fossils (including ours), namely as members of lineages, rather than minimum age priors for discrete MRCA. To avoid over-interpretation of the fossils during the latter, all fossil age constraints and estimates were used here in a conservative manner (see Descriptions; Inferences). More precise estimates and a larger taxon set would be needed to reconstruct explicit migration pathways of the different Loranthaceae lineages that consider the fossil record of the family.

Timing of evolution of main Loranthaceae lineages

The main, currently aerial parasitic lineages, of Loranthaceae evolved about 20 myrs earlier (Table 3) than estimated by *Vidal-Russell & Nickrent (2008b)*; a discrepancy easily explained. In contrast to the earlier study, we can exclusively rely on ingroup fossils as age constraints, which provide direct evidence for the occurrence of several Loranthaceae lineages in the middle Eocene. *Vidal-Russell & Nickrent (2008b)* used two sets of fossil constraints for their dating of an all-Santalales dataset. The first set used a single fossil (*Anacolosidites* Cookson & K.Pike) to constrain the root age of an Olacaceae s.l. subclade, the former Anacolosideae (= Aptandraceae), to 70 Ma, providing generally older estimates than the second, preferred set. The second set used five additional fossils and included *Cranwellia* Sat.K.Srivast. to constrain the root age of Loranthaceae to >70 Ma. We again diverged from *Vidal-Russell & Nickrent (2008b)*, by not using a different study, i.e. *Wikström, Savolainen & Chase (2001)*, to constrain the (ingroup) root age. Using secondary dating constraints and age priors based on outgroup fossils typically leads to overly young age estimates (e.g. *Grimm & Renner, 2013*, for Betulaceae; *Garzón-Orduña et al., 2015*, for Solanaceae and Ithomiini; *Schenk, 2016*, for simulated data). For example, in the two families of Canellales, namely Canellaceae and Winteraceae, crown group estimates using ingroup fossils as age priors are about double the age of those inferred based on a large magnoliid dataset including only root age constraints for the Winteraceae and the order (*Marquínez et al., 2009*; *Thomas et al., 2014*; *Massoni, Couvreur & Sauquet, 2015*; *Müller et al., 2015*).

It must be noted that the existence of a lineage, as evidenced by the pollen record, does not allow for conclusions to be drawn regarding the parasitic habit of its extinct members. The *Muellerina–Gaiadendron* case shows that root and aerial parasites produce similar pollen grains. Even if we consider this pollen type to be primitive ('symplesiomorphic'), the shift of the Lorantheae to aerial parasitism did not affect the pollen morphology in all of its sublineages to the same degree. The unconstrained topologies indicate several shifts from root to aerial parasitism within the family. It may thus be possible that more

shifts occurred in the past than visible from the present-day situation. Ancient members of a Loranthaceae lineage may have been root parasites (or intermediate) in contrast to their modern representatives. Our older estimates nevertheless make sense considering the substantial genetic divergence between extant Loranthaceae, the backdrop of Cenozoic global climate evolution, and the evolutionary history of the potential hosts for aerial Loranthaceae: mid- to high-canopy trees (see also Fig. 8). Although some species of the Loranthaceae family seem to be linked to a specific host, the genera themselves usually parasitise a wide range of hosts, spanning different families and even orders (File S6). The colonisation potential of aerial mistletoes is high. For instance, the New Zealand endemic *Ileostylus micranthus* (Lorantheae: Ileostylinae) parasitises 47 different families, including northern hemispheric lineages introduced in historic times (*Norton & de Lange, 1999*). Australian mistletoes commonly infest two widespread, common and native tree genera (*Acacia, Eucalyptus*), but in total 256 genera are infested, and species of four genera can be found on exotic (introduced) tree genera such as *Nerium*, *Quercus* (oaks), *Platanus*, and *Salix*, among others (*Downey, 1998*). All these genera are potential hosts of northern hemispheric Loranthaceae (e.g. *Loranthus europaeus*), and can be traced back at least to the Eocene (e.g. *Mai, 1995*). For example, primary radiation and diversification of oaks—the most diverse, extratropical tree genus of the Northern Hemisphere with more than 400 modern species (*Nixon, 1997*; *Huang, Zhang & Bartholomew, 1999*)—was finished by the end of the Eocene (*Hubert et al., 2014*). The general vegetation types in which aerial Loranthaceae are found—various sorts of subtropical to temperate, non-frost forests but also tropical biomes—have been available through the entire Cenozoic (e.g. *Mai, 1995*). Most of the Eocene is characterised by a globally ameliorated climate (*Zachos et al., 2001*). During this time scale, tropical and subtropical forests reached a peak in their distribution, with subtropical and temperate forests reaching far north. This could have been the trigger for a global radiation of aerial parasites in Loranthaceae. In western Greenland, currently epiphytic Loranthaceae (Psittacanthinae; Aamaruutissaa MT, aff. *Tripodanthus*) co-occurred with a high variety of subtropical to temperate Fagaceae including various intrageneric groups of oaks (*Grímsson et al., 2015*). Fagaceae in general (see File S6) and oaks in particular are natural hosts of Eurasian Lorantheae. Oaks are major elements of extratropical northern hemispheric mid- to high-canopy forests and open woodlands. The Aamaruutissaa palynological assemblage covers representatives of ca. 30 families of woody angiosperms in total (*Grímsson et al., 2014b*), including many potential hosts of epiphytic Loranthaceae in modern-day extra-tropical North America and East Asia. The arborescent families Fagaceae, Juglandaceae, and Sapindaceae (including maples, *Acer*) can be found at all other localities included in our study (Table 1; File S7). All LM/SEM palynologically studied floras further comprise lianas (Vitaceae) and additional predominately or exclusively arborescent families such as Aquifoliaceae (*Ilex*), Cornaceae, Malvaceae, Myricaceae, Oleaceae, Platanaceae, and Ulmaceae. On the other hand, typically or exclusively herbaceous families are rare (or absent). Thus, the early Loranthaceae described here apparently thrived in densely forested habitats with ample niche opportunities for aerial parasites.

The mid-Oligocene falls into a phase of global cooling and retreat of subtropical and tropical vegetation belts to lower latitudes. If the main currently aerial parasitic lineages evolved during that time in Australia, as inferred by *Vidal-Russell & Nickrent (2008a*, *2008b*; but see *Barlow, 1990*; *Vidal-Russell & Nickrent, 2007)*, Loranthaceae would have needed to be extremely competitive to radiate at a global scale. With its (cold-)temperate to polar climate from the Oligocene onwards, Antarctica is an unlikely corridor for the global radiation of Loranthaceae. The situation in eastern North America and Europe, two areas heavily affected by the Pleistocene climate fluctuations, indicates that Loranthaceae cannot compete with their distant sister clade Viscaceae in the temperate zone, and there is no indication that any Loranthaceae lineage ever thrived in cold-temperate (boreal) climates. Long-distance dispersal via Africa or the Pacific is unlikely in the light of the modern distribution patterns (Fig. 11). All continental African species are members of the core Lorantheae, and distant relatives of the exclusively Australasian and South American lineages. The age estimates indicate that main Australasian (probably monophyletic Elytrantheae) and New World lineages (probably paraphyletic Psittacantheae) diverged around the same time (Fig. 8; Table 3), which would fit with the traditional Gondwana-Breakup scenario suggested for the family (*Barlow, 1990*; *Vidal-Russell & Nickrent, 2007*). Whether divergences in Loranthaceae are triggered by actual tectonic events has to be tested once a more comprehensive taxon and gene sample is available, and would require a re-investigation of the pollen record of the Southern Hemisphere using combined LM and SEM microscopy. With such data at hand, explicit pollen evolution scenarios could be established to discriminate between pollen indicative of ancestral or deep-rooting, slow-evolving (regarding their pollen morphologies) modern lineages, and extant genera or relatively late radiated supergeneric groups. The Oligocene cooling may have been the final trigger to isolate the American lineages from those in the Old World and Australasia. It also may have effected transcontinental exchange between Africa and East Asia, trigger the formation of the contemporary genera (Fig. 9; Table 3, but see the Discussion section), and manifest the isolation of Australasian lineages.

CONCLUSION

Molecular age estimates have often been criticised as being too young in comparison to the fossil record. The crown group radiation and associated onset of aerial parasitism in Loranthaceae, placed in the middle Oligocene by a study including all lineages of the Santalales (*Vidal-Russell & Nickrent, 2008b*), could have been taken for such a case. It would have invoked three difficult-to-understand phenomena: (1) Quick long-distance dispersal and rapid radiation on a global scale of a mostly tropical-subtropical lineage during a phase of global cooling; (2) Host-specialisation and simultaneous colonisation of subtropical forest elements that were already evolved by the Eocene, at least 20 myrs earlier; (3) The comparatively rich palynological record of the zoophilous Loranthaceae, with earliest reliable records in the Eocene of Australasia (south-eastern Australia, Tasmania), East Asia (Hainan, southern China), western Eurasia (Germany), the Americas (Argentina, southeastern United States) and Greenland reflect a largely lost diversity of root parasites or extinct sister lineages of extant Loranthaceae. These extinct lineages

would then have been replaced, at the earliest, in the middle Oligocene (except for three refugia) in their entire range by their newly evolved aerial parasitic siblings. Using SEM-studied fossil pollen, we can push back the origin(s) of the main Loranthaceae lineages to at least the middle Eocene; a time when important hosts of modern epiphytic Loranthaceae evolved and radiated, and Earth enjoyed a phase of ameliorated climate. The new dating estimates are furthermore relatively stable regarding alternative rooting scenarios for the family.

ACKNOWLEDGEMENTS

Ignacio Escapas and Benjamin Bomfleur are thanked for supplying South American literature, Kanchi Natarajan Gandhi from the IPNI team for clarifying the standard author form for the Indian palynologist Satish Srivastava, Marco Simeone for providing a compilation of plastid substitution rates reported in literature, and two anonymous reviewers and the editor for their constructive comments on the manuscript. Alastair Potts and Maxine Smit are acknowledged for proof-reading the original submission and final manuscript.

ADDITIONAL INFORMATION AND DECLARATIONS

Funding

This study was funded by the Austrian Science Fund (FWF) with grants to FG, project number P24427-B25, and GWG, project number M1751-B16, and by Synthesis FP7–the European Union-funded Integrated Activities Grants DK-TAF 1971, SE-TAF 1918, and GB-TAF 3740 to FG. The funders had no role in study design, data collection and analysis, decision to publish, or preparation of the manuscript.

Grant Disclosures

The following grant information was disclosed by the authors:
Austrian Science Fund (FWF): P24427-B25 and M1751-B16.
Synthesis FP7–the European Union-funded Integrated Activities: DK-TAF 1971, SE-TAF 1918, and GB-TAF 3740.

Competing Interests

The authors declare that they have no competing interests.

Author Contributions

- Friðgeir Grímsson conceived and designed the experiments, performed the experiments, contributed reagents/materials/analysis tools, wrote the paper, prepared figures and/or tables, reviewed drafts of the paper, and provided artwork (pollen plates); processed of samples and identification and taxonomic description of pollen types.
- Paschalia Kapli conceived and designed the experiments, performed the experiments, analysed the data, contributed reagents/materials/analysis tools, reviewed drafts of the paper.

- Christa-Charlotte Hofmann contributed reagents/materials/analysis tools, reviewed drafts of the paper, processed of samples and identification and taxonomic description of pollen types.
- Reinhard Zetter contributed reagents/materials/analysis tools, reviewed drafts of the paper, processed of samples and identification and taxonomic description of pollen types.
- Guido W. Grimm conceived and designed the experiments, performed the experiments, analysed the data, contributed reagents/materials/analysis tools, wrote the paper, prepared figures and/or tables, reviewed drafts of the paper, and created artwork (other than pollen plates); compiled online supporting archive.

Supplemental Information

Supplemental information for this article can be found online at http://dx.doi.org/10.7717/peerj.3373#supplemental-information.

REFERENCES

Amico GC, Vidal-Russell R, Garcia MA, Nickrent DL. 2012. Evolutionary history of the South American mistletoe *Tripodanthus* (Loranthaceae) using nuclear and plastid markers. *Systematic Botany* **37(1)**:218–225 DOI 10.1600/036364412x616783.

Baele G, Lemey P, Bedford T, Rambaut A, Suchard MA, Alekseyenko AV. 2012. Improving the accuracy of demographic and molecular clock model comparison while accommodating phylogenetic uncertainty. *Molecular Biology and Evolution* **29(9)**:2157–2167 DOI 10.1093/molbev/mss084.

Baele G, Li WLS, Drummond AJ, Suchard MA, Lemey P. 2013. Accurate model selection of relaxed molecular clocks in bayesian phylogenetics. *Molecular Biology and Evolution* **30(2)**:239–243 DOI 10.1093/molbev/mss243.

Barlow BA. 1990. Biogeographical relationships of Australia and Malesia: Loranthaceae as a model. In: Baas P, Kalkmann K, Geesink R, eds. *The Plant Diversity of Malesia*. Dordrecht, Boston, London: Kluwer Academic Publishers, pp. 273–292.

Bartlett AS, Barghoorn ES. 1973. Phytogeographic history of the Isthmus of Panama during the past 12,000 years (a history of vegetation, climate, and sea-level change). In: Graham A, ed. *Vegetation and Vegetational History of Northern Latin America*. Amsterdam: Elsevier Science Publishers, 203–299.

Blakey RC. 2008. Gondwana paleogeography from assembly to breakup—A 500 m.y. odyssey. In: Fielding CR, Frank TD, Isbell JL, eds. *Resolving the Late Paleozoic Ice Age in Time and Space*. Boulder: Geological Society of America, pp. 1–28.

Bouchal JM, Zetter R, Denk T. 2016. Pollen and spores of the uppermost Eocene Florissant Formation, Colorado: a combined light and scanning electron microscopy study. *Grana* **55**:179–245.

Caires CS. 2012. Estudos taxonômicos aprofundados de O*ryctanthus* (Griseb.) Eichler, O*ryctina* T*iegh*, e P*usillanthus K*uijt (Loranthaceae). Ph.D. Thesis. Universidade de Brasília.

Chen S-C, Zhang L, Zeng J, She F, Yang H, Mao Y-R, Fu C-X. 2012. Geographic variation of chloroplast DNA in *Platycarya strobilacea* (Juglandaceae). *Journal of Systematics and Evolution* **50(4)**:374–385 DOI 10.1111/j.1759-6831.2012.00210.x.

Cohen KM, Finney SC, Gibbard PL, Fan J-X. 2013 (updated). The ICS International Chronostratigraphic Chart. *Episodes* **36**:199–204.

Dam G, Pedersen GK, Sønderholm M, Midtgaard HH, Larsen LM, Nøhr-Hansen H, Pedersen AK. 2009. Lithostratigraphy of the Cretaceous–Paleocene Nuussuaq Group, Nuussuaq Basin, West Greenland. *Geological Survey of Denmark and Greenland Bulletin* **19**:1–171.

Darriba D, Taboada GL, Doallo R, Posada D. 2012. jModelTest 2: more models, new heuristics and parallel computing. *Nature Methods* **9(8)**:772–772 DOI 10.1038/nmeth.2109.

del Carmen Zamaloa M, Fernández CA. 2016. Pollen morphology and fossil record of the feathery mistletoe family Misodendraceae. *Grana* **55(4)**:278–285 DOI 10.1080/00173134.2015.1120776.

Désamoré A, Laenen B, Devos N, Popp M. 2011. Out of Africa: north-westwards Pleistocene expansions of the heather *Erica arborea*. *Journal of Biogeography* **38(1)**:164–176 DOI 10.1111/j.1365-2699.2010.02387.x.

Dilcher DL, Lott TA. 2005. A middle Eocene fossil plant assemblage (Power Clay Pit) from western Tennessee. *Bulletin of the Florida Museum of Natural History* **45**:1–43.

Dornburg A, Brandley MC, McGowen MR, Near TJ. 2012. Relaxed clocks and inferences of heterogeneous patterns of nucleotide substitution and divergence time estimates across whales and dolphins (Mammalia: Cetacea). *Molecular Biology and Evolution* **29(2)**:721–736 DOI 10.1093/molbev/msr228.

Downey PO. 1998. An inventory of host species for each aerial mistletoe species (Loranthaceae and Viscaceae) in Australia. *Cunninghamia* **5**:685–719.

Drummond AJ, Rambaut A. 2007. BEAST: Bayesian evolutionary analysis by sampling trees. *BMC Evolutionary Biology* **7(1)**:214 DOI 10.1186/1471-2148-7-214.

Drummond AJ, Suchard MA, Xie D, Rambaut A. 2012. Bayesian phylogenetics with BEAUti and the BEAST 1.7. *Molecular Biology and Evolution* **29(8)**:1969–1973 DOI 10.1093/molbev/mss075.

Engelhardt H. 1870. *Flora der Braunkohlenformation im Königreich Sachsen. Preisschrift von der Jablonowyn'schen Gesellschaft. Mit einer Mappe enthaltend fünfzehn Tafeln.* Leipzig: S. Hirzel.

Eschig M. 1992. Zur Florenentwicklung und Stratigraphie im Mitteloligozän der Kremser Bucht, NÖ, Österreich. MSc thesis. University of Vienna.

Ferguson DK, Lee DE, Bannister JM, Zetter R, Jordan GJ, Vavra N, Mildenhall DC. 2009. The taphonomy of a remarkable leaf bed assemblage from the Late Oligocene–Early Miocene Gore Lignite Measures, southern New Zealand. *International Journal of Coal Geology* **83(2–3)**:173–181 DOI 10.1016/j.coal.2009.07.009.

Feuer SM. 1977. Pollen Morphology and Evolution in the Santalales sen. str., a Parasitic Order of Flowering Plantsthesis. Ph.D. thesis. University of Massachusetts.

Feuer SM. 1978. Aperture evolution in the genus *Ptychopetalum* Benth. (Olacaceae). *American Journal of Botany* **65(7)**:759–763 DOI 10.2307/2442151.

Feuer SM. 1981. Pollen morphology and relationships of the Misodendraceae (Santalales). *Nordic Journal of Botany* **1(6)**:731–734 DOI 10.1111/j.1756-1051.1981.tb01159.x.

Feuer SM, Kuijt J. 1978. Fine structure of mistletoe pollen I. Eremolepidaceae, *Lepidoceras*, and *Tupeia*. *Canadian Journal of Botany* **56(22)**:2853–2864 DOI 10.1139/b78-341.

Feuer SM, Kuijt J. 1979. Pollen evolution in the genus *Psittacanthus* Mart. Fine structure of mistletoe pollen II. *Botaniska Notiser* **132**:295–309.

Feuer SM, Kuijt J. 1980. Fine structure of mistletoe pollen III. Large-flowered neotropical Loranthaceae and their Australian relatives. *Annals of the Missouri Botanical Garden* **72**:187–212.

Feuer SM, Kuijt J. 1982. Fine structure of mistletoe pollen IV. Eurasian and Australian *Viscum* L. (Viscaceae). *American Journal of Botany* **69(1)**:1–12 DOI 10.2307/2442826.

Feuer SM, Kuijt J. 1985. Fine structure of mistletoe pollen VI. Small-flowered neotropical Loranthaceae. *Annals of the Missouri Botanical Garden* **72(2)**:187–212 DOI 10.2307/2399176.

Feuer SM, Kuijt J, Wiens D. 1982. Fine structure of mistletoe pollen V. Madagascan and continental African *Viscum* L. (Viscaceae). *American Journal of Botany* **69(2)**:163–187 DOI 10.2307/2443005.

Garzón-Orduña IJ, Silva-Brandão KL, Willmott KR, Freitas AVL, Brower AVZ. 2015. Incompatible ages for clearwing butterflies based on alternative secondary calibrations. *Systematic Biology* **64(5)**:752–767 DOI 10.1093/sysbio/syv032.

Göker M, Grimm GW. 2008. General functions to transform associate data to host data, and their use in phylogenetic inference from sequences with intra-individual variability. *BMC Evolutionary Biology* **8(1)**:86 DOI 10.1186/1471-2148-8-86.

Graham A. 1990. Late Tertiary microfossil flora from the Republic of Haiti. *American Journal of Botany* **77(7)**:911–926 DOI 10.2307/2444507.

Gregor H-J. 2005. Pflanzen und Tiere aus den eozänen Braunkohlen des Untertagebaues Stolzenbach bei Kassel. *Philippia* **12**:147–181.

Gregor H-J, Oschkinis V. 2013. Die eozänen Braunkohleschichten aus dem Untertagebau Stolzenbach bei Kassel (PreußenElektra, Niederhessen) XI. Die tierischen Reste—Insekten. *Documenta naturae* **193**:51–56.

Grimm GW, Kapli P, Bomfleur B, McLoughlin S, Renner SS. 2015. Using more than the oldest fossils: Dating Osmundaceae with the fossilized birth-death process. *Systematic Biology* **64**:396–405.

Grimm GW, Renner SS. 2013. Harvesting GenBank for a Betulaceae supermatrix, and a new chronogram for the family. *Botanical Journal of the Linnéan Society* **172(4)**:465–477 DOI 10.1111/boj.12065.

Grimm GW, Renner SS, Stamatakis A, Hemleben V. 2006. A nuclear ribosomal DNA phylogeny of *Acer* inferred with maximum likelihood, splits graphs, and motif analyses of 606 sequences. *Evolutionary Bioinformatics* **2**:279–294.

Grímsson F, Denk T, Zetter R. 2008. Pollen, fruits, and leaves of *Tetracentron* (Trochodendraceae) from the Cainozoic of Iceland and western North America and their palaeobiogeographic implications. *Grana* **47(1)**:1–14 DOI 10.1080/00173130701873081.

Grímsson F, Zetter R, Hofmann C-C. 2011. *Lythrum* and *Peplis* from the Late Cretaceous and Cenozoic of North America and Eurasia: new evidence suggesting early diversification within the Lythraceae. *American Journal of Botany* **98(11)**:1801–1815 DOI 10.3732/ajb.1100204.

Grímsson F, Ferguson DK, Zetter R. 2012. Morphological trends in the fossil pollen of *Decodon* and the paleobiogeographic history of the genus. *International Journal of Plant Sciences* **173(3)**:297–317 DOI 10.1086/663968.

Grímsson F, Zetter R, Halbritter H, Grimm GW. 2014a. *Aponogeton* pollen from the Cretaceous and Paleogene of North America and West Greenland: Implications for the origin and palaeobiogeography of the genus. *Review of Palaeobotany and Palynology* **200**:161–187 DOI 10.1016/j.revpalbo.2013.09.005.

Grímsson F, Zetter R, Pedersen GK, Pedersen AK, Denk T. 2014b. Middle Eocene palaeoflora from a resinite-rich coal bed on Hareøn (Qeqertarsuatsiag), West Greenland. *9th European Palaeobotany—Palynology Conference EPPC2014, Padova,* p. 86 [abstract].

Grímsson F, Zetter R, Grimm GW, Krarup Pedersen G, Pedersen AK, Denk T. 2015. Fagaceae pollen from the early Cenozoic of West Greenland: revisiting Engler's and Chaney's Arcto-Tertiary hypotheses. *Plant Systematics and Evolution* **301(2)**:809–832 DOI 10.1007/s00606-014-1118-5.

Grímsson F, Grimm GW, Zetter R, Denk T. 2016. Cretaceous and Paleogene Fagaceae from North America and Greenland: evidence for a Late Cretaceous split between *Fagus* and the remaining Fagaceae. *Acta Palaeobotanica* **56(2)**:247–305 DOI 10.1515/acpa-2016-0016.

Grímsson F, Grimm GW, Zetter R. 2017. Evolution of pollen morphology in Loranthaceae. *Grana* DOI 10.1080/00173134.2016.1261939 [Epub ahead of print 20 Feb 2017].

Guo S-X. 1979. Late Cretaceous and Early Tertiary floras from the southern Guangdong and Guangxi with their stratigraphic significance [in Chinese]. In: Institute of Vertebrate Palaeontology and Palaeoanthropology, Nanjing Institute of Geology and Palaeontology, and Academia Sinica, ed. *Mesozoic and Cenozoic Red Beds of South China*. Bejing: Science Press, 223–230.

Guzmán B, Vargas P. 2010. Unexpected synchronous differentiation in Mediterranean and Canarian *Cistus* (Cistaceae). *Perspectives in Plant Ecology, Evolution and Systematics* **12(3)**:163–174 DOI 10.1016/j.ppees.2009.09.002.

Hald N. 1976. Early Tertiary flood basalts from Hareøen and western Nûgssuaq, West Greenland. *Grønlands Geologiske Undersøgelse Bulletin* **120**:1–36.

Hald N. 1977. Lithostratigraphy of the Maligât and Hareøen Formations, West Greenland Basalt Group, on Hareøen and western Nûgssuaq. *Rapport Grønlands Geologiske Undersøgelse* **79**:9–16.

Han R-L, Zhang D-X, Hao G. 2004. Pollen morphology of the Loranthaceae from China. *Acta Phytotaxonomica Sinica* **42**:436–456.

Heath TA, Huelsenbeck JP, Stadler T. 2014. The fossilized birth–death process for coherent calibration of divergence-time estimates. *Proceedings of the National Academy of Sciences of the United States of America* **111(29)**:E2957–E2966 DOI 10.1073/pnas.1319091111.

Heer O. 1883. *Flora fossilis arctica 7. Die fossile Flora der Polarländer. Enthaltend: Den zweiten Theil der fossilen Flora Grönlands.* Zürich: J. Wurster & Comp.

Hochuli PA. 1978. Palynologische Untersuchungen im Oligozän und Untermiozän der Zentralen und Westlichen Paratethys. *Beiträge zur Paläontologie Österreichs* **4**:1–132.

Holland B, Moulton V. 2003. Consensus networks: a method for visualising incompatibilities in collections of trees. In: Benson G, Page R, eds. *Algorithms in Bioinformatics: Third International Workshop, WABI, Budapest, Hungary Proceedings.* Berlin: Springer, pp. 165–176.

Hottenrott M, Gregor H-J, Oschkinis V. 2010. Die eozäne Braunkohleschichten aus dem Untertagebau Stolzenbach bei Kassel (PreußenElektra, Niederhessen) VII. Die Mikroflora. *Documenta Naturae* **181**:29–43.

Huang C, Zhang Y, Bartholomew B. 1999. Fagaceae. In: Wu Z-Y, Raven PH, eds. *Flora of China 4 Cycadaceae through Fagaceae.* Beijing, St. Louis: Science Press and Missouri Botanical Garden Press.

Hubert F, Grimm GW, Jousselin E, Berry V, Franc A, Kremer A. 2014. Multiple nuclear genes stabilize the phylogenetic backbone of the genus *Quercus*. *Systematics and Biodiversity* **12(4)**:405–423 DOI 10.1080/14772000.2014.941037.

Huelsenbeck JP, Bollback JP, Levine AM. 2002. Inferring the root of a phylogenetic tree. *Systematic Biology* **51(1)**:32–43 DOI 10.1080/106351502753475862.

Huson DH, Bryant D. 2006. Application of phylogenetic networks in evolutionary studies. *Molecular Biology and Evolution* **23(2)**:254–267 DOI 10.1093/molbev/msj030.

Jin J-H, Liao W-B, Wang B-S, Peng S-L. 2002. Palaeodiversification of the environment and plant community of Tertiary in Hainan Island [in Chinese with English abstract]. *Acta Ecologica Sinica* **22**:425–432.

Kass RE, Raftery AE. 1995. Bayes factors. *Journal of the American Statistical Association* **90**:773–795.

Kmenta M. 2011. Die Mikroflora der untermiozänen Fundstelle Altmittweida, Deutschland. MSc thesis. University of Vienna.

Kmenta M, Zetter R. 2013. Combined LM and SEM study of the upper Oligocene/lower Miocene palynoflora from Altmittweida (Saxony): Providing new insights into Cenozoic vegetation evolution of Central Europe. *Review of Palaeobotany and Palynology* **195**:1–18 DOI 10.1016/j.revpalbo.2013.03.007.

Krutzsch W, Lenk G. 1973. Sporenpaläontologische Untersuchungen im Alttertiär des Weißelster-Beckens. I. Die stratigraphisch wichtigen Pollen- und Sporenformen aus dem Profil des Tagebaus Profen. *Abhandlungen des Zentralen Geologischen Instituts* **18**:59–76.

Kuijt J. 1988. Revision of *Tristerix* (Loranthaceae). *Systematic Botany Monographs* **19**:1–61 DOI 10.2307/25027693.

Kuijt J. 2011. Pulling the skeleton out of the closet: resurrection of *Phthirusa* sensu Martius and consequent revival of *Passovia* (Loranthaceae). *Plant Diversity and Evolution* **129(2)**:159–211 DOI 10.1127/1869-6155/2011/0129-0049.

Larsen LM, Pedersen AK, Tegner C, Duncan RA, Hald N, Larsen JG. 2015. The age of Tertiary volcanic rocks on the West Greenland continental margin: volcanic evolution and event correlation to other parts of the North Atlantic Igneous Province. *Geological Magazine* **153(3)**:487–511 DOI 10.1017/s0016756815000515.

Lei YZ, Zhang QR, He W, Cao XP. 1992. Tertiary. In: Wang XF, ed. *Geology of Hainan Island I Stratigraphy and Palaeontology [in Chinese]*. Beijing: Geological Publishing House, pp. 218–266.

Liu L-F, Qiu H-X. 1993. Pollen morphology of Loranthaceae in China [in Chinese with English abstract]. *Guihaia* **13**:235–245.

Lockwood JD, Aleksić JM, Zou J, Wang J, Liu J, Renner SS. 2013. A new phylogeny for the genus *Picea* from plastid, mitochondrial, and nuclear sequences. *Molecular Phylogenetics and Evolution* **69(3)**:717–727 DOI 10.1016/j.ympev.2013.07.004.

Macphail MK, Jordan GJ, Hopf F, Colhoun EA. 2012. When did the mistletoe family Loranthaceae become extinct in Tasmania? Review and conjecture. *Terra Australis* **34**:255–269.

Maddison WP, Maddison DR. 2011. Mesquite: a modular system for evolutionary analysis. Version 2.75. *Available at http://mesquiteproject.org*.

Maguire B, Wurdack JJ, Huang Y-C. 1974. Pollen grains of some American Olacaceae. *Grana* **14(1)**:26–38 DOI 10.1080/00173137409434771.

Mai DH. 1995. *Tertiäre Vegetationsgeschichte Europas*. Jena, Stuttgart, New York: Gustav Fischer Verlag.

Mai DH, Walther H. 1991. Die oligozänen und untermiozänen Floren NW-Sachsens und des Bitterfelder Raumes. *Abhandlungen des Staatlichen Museum für Mineralogie und Geologie Dresden* **38**:1–230.

Manchester SR, Grímsson F, Zetter R. 2015. Assessing the fossil record of asterids in the context of our current phylogenetic framework. *Annals of the Missouri Botanical Garden* **100(4)**:329–363 DOI 10.3417/2014033.

Marquínez X, Lohmann LG, Salatino MLF, Salatino A, González F. 2009. Generic relationships and dating lineages in Winteraceae based on nuclear (ITS) and plastid (rpS16 and psbA-trnH) sequence data. *Molecular Phylogenetics and Evolution* **53(2)**:435–449 DOI 10.1016/j.ympev.2009.07.001.

Massoni J, Couvreur TLP, Sauquet H. 2015. Five major shifts of diversification through the long evolutionary history of Magnoliidae (angiosperms). *BMC Evolutionary Biology* **15(1)**:49 DOI 10.1186/s12862-015-0320-6.

Muller J. 1981. Fossil pollen records of extant angiosperms. *Botanical Review* **47(1)**:1–142 DOI 10.1007/bf02860537.

Müller S, Salomo K, Salazar J, Naumann J, Jaramillo MA, Neinhuis C, Feild TS, Wanke S. 2015. Intercontinental long-distance dispersal of Canellaceae from the New to the Old World revealed by a nuclear single copy gene and chloroplast loci. *Molecular Phylogenetics and Evolution* **84**:205–219 DOI 10.1016/j.ympev.2014.12.010.

Nickrent DL. 1997 onwards. *The Parasitic Plant Connection. Available at http://parasiticplants.siu.edu* (accessed 18 April 2016).

Nickrent DL, Malécot V, Vidal-Russell R, Der JP. 2010. A revised classification of Santalales. *Taxon* **9**:538–558.

Nixon KC. 1997. Fagaceae. In: Flora of North America Editorial Committee, ed. *Flora of North America North of Mexico*. New York: Oxford University Press, 436–537.

Norton DA, de Lange PJ. 1999. Host specifity in parasitic mistletoes (Loranthaceae) in New Zealand. *Functional Ecology* **13(4)**:552–559 DOI 10.1046/j.1365-2435.1999.00347.x.

Oschkinis V, Gregor H-J. 1992. Paläontologische Funde aus der eozänen Braunkohle des Untertagebaus Stolzenbach (PreußenElektra) in Niederhessen—I. Die Flora. *Documenta Naturae* **72**:1–31.

Pälchen W, Walter H. 2011. *Geologie von Sachsen I. Geologischer Bau und Entwicklungsgeschichte. 2. Auflage*. Stuttgart: E. Schweizerbart'sche Verlagsbuchhandlung.

Palmer JD. 1991. Plastid chromosomes: structure and evolution. In: Bogorad L, Vasil IK, eds. *The Molecular Biology of Plastids*. San Diego: Academic Press, Inc., pp. 5–55.

Pattengale ND, Masoud A, Bininda-Emonds ORP, Moret BME, Stamatakis A. 2009. How many bootstrap replicates are necessary? In: Batzoglou S, ed. *RECOMB 2009*. Berlin: Springer-Verlag, pp. 184–200.

Potter FWJ. 1976. Investigations of angiosperms from the Eocene of southeastern North America: Pollen assemblages from Miller Pit, Henry County, Tennessee. *Palaeontographica, Abteilung B* **157**:44–96.

Punt W, Hoen PP, Blackmore S, Nilsson S, Le Thomas A. 2007. Glossary of pollen and spore terminology. *Review of Palaeobotany and Palynology* **143(1–2)**:1–81 DOI 10.1016/j.revpalbo.2006.06.008.

Renner SS, Grimm GW, Schneeweiss GM, Stuessy TF, Ricklefs RE. 2008. Rooting and dating maples (*Acer*) with an uncorrelated-rates molecular clock: implications for North American/Asian disjunctions. *Systematic Biology* **57(5)**:795–808 DOI 10.1080/10635150802422282.

Renner SS, Grimm GW, Kapli P, Denk T. 2016. Species relationships and divergence times in beeches: New insights from the inclusion of 53 young and old fossils in a birth-death clock model. *Philosophical Transactions of the Royal Society B: Biological Sciences* **371(1699)**:20150135 DOI 10.1098/rstb.2015.0135.

Roldán FJ, Kuijt J. 2005. A new, red-flowered species of *Tripodanthus* (Loranthaceae) from Columbia. *Novon* **15**:207–209.

Schenk JJ. 2016. Consequences of secondary calibrations on divergence time estimates. *PLoS ONE* **11(1)**:e0148228 DOI 10.1371/journal.pone.0148228.

Schmidt AG, Riisager P, Abrahamsen N, Riisager J, Pedersen AK, van der Voo R. 2005. Palaeomagnetism of Eocene Talerua Member lavas on Hareøen, West Greenland. *Bulletin of the Geological Society of Denmark* **52**:27–38.

Smith SA, Beaulieu JM, Donoghue MJ. 2009. An uncorrelated relaxed-clock analysis suggests an earlier origin for flowering plants. *Proceedings of the National Academy of Sciences of the United States of America* **107(13)**:5897–5902 DOI 10.1073/pnas.1001225107.

Smith SA, Donoghue MJ. 2008. Rates of molecular evolution are linked to life history in flowering plants. *Science* **322(5898)**:86–89 DOI 10.1126/science.1163197.

Song Z-C, Wang W-M, Huang F. 2004. Fossil pollen records of extant angiosperms in China. *Botanical Review* **70(4)**:425–458 DOI 10.1663/0006-8101(2004)070[0425:fproea]2.0.co;2.

Spicer RA, Herman AB, Liao W, Spicer TEV, Kodrul TM, Yang J, Jin J. 2014. Cool tropics in the Middle Eocene: Evidence from the Changchang Flora, Hainan Island, China. *Palaeogeography, Palaeoclimatology, Palaeoecology* **412**:1–16 DOI 10.1016/j.palaeo.2014.07.011.

Stamatakis A. 2014. RAxML version 8: a tool for phylogenetic analysis and post-analysis of large phylogenies. *Bioinformatics* **30(9)**:1312–1313 DOI 10.1093/bioinformatics/btu033.

Standke G. 2008. Tertiär. In: Pälchen W, Walter H, eds. *Geologie von Sachsen Geologischer Bau und Entwicklungsgeschichte*. Stuttgart: E. Schweizerbart'sche Verlagsbuchhandlung, pp. 358–419.

Su H-J, Hu J-M, Anderson FE, Der JP, Nickrent DL. 2015. Phylogenetic relationships of Santalales with insights into the origins of holoparasitic Balanophoraceae. *Taxon* **64(3)**:491–506 DOI 10.12705/643.2.

Taylor DW. 1989. Selected palynomorphs from the middle Eocene Claiborne Formation, Tenn., (U.S.A.). *Review of Palaeobotany and Palynology* **58(2–4)**:111–128 DOI 10.1016/0034-6667(89)90080-8.

Thomas N, Bruhl JJ, Ford A, Weston PH. 2014. Molecular dating of Winteraceae reveals a complex biogeographical history involving both ancient Gondwanan vicariance and long-distance dispersal. *Journal of Biogeography* **41(5)**:894–904 DOI 10.1111/jbi.12265.

Tropicos.org. 2016. *Tropicos® Database*. St. Louis: Missouri Botanical Garden. *Available at http://www.tropicos.org* (accessed 19 May 2016).

Tschudy RH. 1973. Stratigraphic distribution of significant Eocene palynomorphs of the Mississippi embayment. *US Geological Survey Professional Paper* **743-B**:B1–B24.

Vidal-Russell R, Nickrent DL. 2007. The biogeographic history of Loranthaceae. *Darwiniana* **45**:52–54.

Vidal-Russell R, Nickrent DL. 2008a. Evolutionary relationships in the showy mistletoe family (Loranthaceae). *American Journal of Botany* **95(8)**:1015–1029 DOI 10.3732/ajb.0800085.

Vidal-Russell R, Nickrent DL. 2008b. The first mistletoes: Origins of aerial parasitism in Santalales. *Molecular Phylogenetics and Evolution* **47(2)**:523–537 DOI 10.1016/j.ympev.2008.01.016.

Wang H, Blanchard J, Dilcher DL. 2013. Fruits, seeds, and flowers from the Warman clay pit (middle Eocene Claiborne Group), western Tennessee, USA. *Palaeontologia Electronica* **16**:31A.

Weber L, Weiss A. 1983. Bergbaugeschichte und Geologie der österreichischen Braunkohlenvorkommen. *Archiv für Lagerstättenforschung der Geologischen Bundesanstalt* **4**:1–317.

Wikström N, Savolainen V, Chase MW. 2001. Evolution of the angiosperms: Calibrating the family tree. *Proceedings of the Royal Society B: Biological Sciences* **268(1482)**:2211–2220 DOI 10.1098/rspb.2001.1782.

Wilson CA, Calvin CL. 2006. An origin of aerial branch parasitism in the mistletoe family, Loranthaceae. *American Journal of Botany* **93(5)**:787–796 DOI 10.3732/ajb.93.5.787.

Wolfe KH, Li W-H, Sharp PM. 1987. Rates of nucleotide substitution vary greatly among plant mitochondrial, chloroplast, and nuclear DNAs. *Proceedings of the National Academy of Sciences of the United States of America* **84(24)**:9054–9058 DOI 10.1073/pnas.84.24.9054.

Yao Y-F, Bera S, Ferguson DK, Mosbrugger V, Paudayal KN, Jin J-H, Li C-S. 2009. Reconstruction of paleovegetation and paleoclimate in the Early and Middle Eocene, Hainan Island, China. *Climate Change* **92(1–2)**:169–189 DOI 10.1007/s10584-008-9457-2.

Zachos JC, Pagani M, Sloan L, Thomas E, Billups K. 2001. Trends, rhythms, and aberrations in global climate 65 Ma to present. *Science* **292(5517)**:686–693 DOI 10.1126/science.1059412.

Zetter R. 1989. Methodik und Bedeutung einer routinemäßig kombinierten lichtmikroskopischen und rasterelektonenmikroskopischen Untersuchung fossiler Mikrofloren. *Courier Forschungsinstitut Senckenberg* **109**:41–50.

Zetter R, Hesse M, Huber KH. 2002. Combined LM, SEM and TEM studies of Late Cretaceous pollen and spores from Gmünd, Lower Austria. *Stapfia* **80**:201–230.